J. Membrane Biol. 207, 69–89 (2005)
DOI: 10.1007/s00232-005-0802-3

The Journal of
Membrane
Biology

Intracellular Mg^{2+} Influences Both Open and Closed Times of a Native Ca^{2+}-activated BK Channel in Cultured Human Renal Proximal Tubule Cells

M. Kubokawa[1], Y. Sohma[2,3], J. Hirano[1], K. Nakamura[1], T. Kubota[2]
[1]Department of Physiology II, School of Medicine, Iwate Medical University, 19-1, Uchimaru, Morioka, 020-8505 Japan
[2]Department of Physiology, Osaka Medical College, 2-7, Daigakumachi, Takatsuki, 569-8686 Japan
[3]John M. Dalton Cardiovascular Research Center, University of Missouri-Columbia, Columbia, MO 65211, USA

Received: 1 December 2004/Revised: 20 October 2005

Abstract. Effects of intracellular Mg^{2+} on a native Ca^{2+}-and voltage-sensitive large-conductance K^+ channel in cultured human renal proximal tubule cells were examined with the patch-clamp technique in the inside-out mode. At an intracellular concentration of Ca^{2+} ($[Ca^{2+}]_i$) of 10^{-5}–10^{-4} M, addition of 1–10 mM Mg^{2+} increased the open probability (P_o) of the channel, which shifted the P_o –membrane potential (V_m) relationship to the negative voltage direction without causing an appreciable change in the gating charge (Boltzmann constant). However, the Mg^{2+}-induced increase in P_o was suppressed at a relatively low $[Ca^{2+}]_i$ ($10^{-5.5}$–10^{-6} M). Dwell-time histograms have revealed that addition of Mg^{2+} mainly increased P_o by extending open times at 10^{-5} M Ca^{2+} and extending both open and closed times simultaneously at $10^{-5.5}$ M Ca^{2+}. Since our data showed that raising the $[Ca^{2+}]_i$ from 10^{-5} to 10^{-4} M increased P_o mainly by shortening the closed time, extension of the closed time at $10^{-5.5}$ M Ca^{2+} would result from the Mg^{2+}-inhibited Ca^{2+}-dependent activation. At a constant V_m, adding Mg^{2+} enhanced the sigmoidicity of the P_o–$[Ca^{2+}]_i$ relationship with an increase in the Hill coefficient. These results suggest that the major action of Mg^{2+} on this channel is to elevate P_o by lengthening the open time, while extension of the closed time at a relatively low $[Ca^{2+}]_i$ results from a lowering of the sensitivity to Ca^{2+} of the channel by Mg^{2+}, which causes the increase in the Hill coefficient.

Key words: Ca^{2+}-activated K^+ channel — Intracellular Mg^{2+} — Open probability — Gating kinetics — Kidney — Proximal tubule

Introduction

The regulation of large-conductance Ca^{2+}-activated K^+ channels (BK channels) essentially depends on both voltage and the intracellular Ca^{2+} concentration ($[Ca^{2+}]_i$) (Marty, 1981; Barrett, Maglby & Pallotta, 1982, Latorre et al., 1989; McManus, 1991). The functional importance of this type of K^+ channel has been proposed in neurons and smooth muscle cells (Robitaille et al., 1993; Brenner et al., 2000a; Pluger et al., 2000). A number of studies have been carried out to clarify the molecular mechanisms by which BK channels are regulated by voltage and Ca^{2+} using cloned channels. The sensitivity to voltage of BK channel gating is thought to arise from a mechanism involving voltage-sensing residues in the S4 segment (Atkinson, Robertson & Ganetzky, 1991; Adelman et al., 1992; Butler et al., 1993; Cui & Aldrich, 2000). As for the sensitivity to Ca^{2+}, it was reported that Ca^{2+} activated the channel via high-affinity Ca^{2+}-binding sites, termed the "Ca^{2+} bowl", located just before the S10 segment near the COOH terminus of the α subunit (Wei et al., 1994; Schreiber & Salkoff, 1997; Schreiber, Yuan & Salkoff, 1999; Bian, Favre & Moczydlowski, 2001). These findings indicate that voltage and Ca^{2+} activate BK channels through distinct mechanisms, as has been demonstrated by applying the patch-clamp technique to BK channels (Cox, Cui & Aldrich, 1997; Cui, Cox & Aldrich, 1997; Horrigan, Cui & Aldrich, 1999), although a recent study has shown that the Ca^{2+}-induced activation of mSlo channels occurred even

M. Kubokawa and Y. Sohma contributed equally to this work.
Correspondence to: M. Kubokawa; email: mkubokaw@iwate-med.ac.jp

when the "Ca^{2+} bowl" was truncated (Piskorowski & Aldrich, 2002).

In addition to voltage and Ca^{2+}, several BK channels are modulated by intracellular Mg^{2+}. One significant effect of Mg^{2+} on BK channels is to reduce single-channel conductance dose- and voltage-dependently (Tabcharani & Misler, 1989; Ferguson, 1991; Zhang, Puil & Mathers, 1995; Morales et al., l996; Wachter & Turnheim, 1996; Bringmann, Faude & Reichenbach, 1997; Kazachenko & Chemeris, 1998). The effect was reproduced with other divalent cations such as Ca^{2+}, Ni^{2+} and Sr^{2+}, suggesting that the blocking effect of Mg^{2+} on conductance was presumably nonspecific (Ferguson, 1991). Another effect Mg^{2+} has on BK channels is to enhance the open probability (P_o) (Golowasch, Kirkwood & Miller, 1986; Squire & Petersen, 1987; Oberhauser, Alvarez & Latorre, 1988; McLamon & Sawyer, 1993; Zhang et al., 1995; Morales et al., 1996; Bringmann et al., 1997; Shi & Cui, 2001; Zhang, Solaro & Lingle, 2001). Several mechanisms by which Mg^{2+} enhances P_o of BK channels have been proposed (Golowasch et al., 1986; Oberhauser et al., 1988; Shi & Cui, 2001; Zhang et al., 2001). Golowasch et al. (1986) reported that Mg^{2+} at an intracellular concentration ($[Mg^{2+}]_i$) of 10 mM raised P_o with an increase in the Hill coefficient for Ca^{2+}-induced activation from 2.0 to 4.2, suggesting that Mg^{2+} revealed multiple Ca^{2+}-binding sites already present in the absence of Mg^{2+} rather than creating additional ones on the protein. Oberhauser et al. (1988) reported similar results. Consequently, they suggested that Mg^{2+} can bind to the channel, which resulted in the unmasking of new Ca^{2+}-binding sites and an increase in P_o in the presence of Ca^{2+}, since Mg^{2+} failed to activate the channel in the absence of Ca^{2+} even when the $[Mg^{2+}]_i$ was raised to 50 mM (Oberhauser et al., 1988).

Recently, Shi and Cui (2001) demonstrated that a low-affinity, divalent cation-binding site that is responsible for the Mg^{2+}-induced activation of channels is located in the amino-terminal core of the mouse Slo 1 (mSlo 1) α subunit. Their report indicates that Mg^{2+} activates the channel independently of the Ca^{2+}-binding sites. Zhang et al. (2001) also demonstrated that Mg^{2+} could activate the BK channel through a Ca^{2+}-independent mechanism, since activation was observed even in the complete absence of Ca^{2+}. Moreover, it was demonstrated that the Mg^{2+}-binding site in the RCK domain, the intracellular motif of the core that immediately follows the activation gate (S6 helix), is distinct from the high-affinity Ca^{2+}-binding site (Shi et al., 2002). Namely, recent studies (Shi & Cui, 200l; Zhang et al., 2001; Shi et al., 2002) strongly suggest that Mg^{2+} could activate the BK channel through a mechanism independent of Ca^{2+}. However, the concept of the Mg^{2+}-induced activation was mainly based on whole-cell clamping studies performed on exogenously expressed cloned channels, and data on the Mg^{2+}-dependent activation of single channels have not been analyzed.

We have studied a native BK channel endogenously expressed in cultured human renal proximal tubule cells (RPTECs) (Hirano et al., 2002), and have recently found that raising the $[Mg^{2+}]_i$ elevates the P_o of this channel by extending open times with a marked reduction in the outward current amplitude. Furthermore, we found that closed times of the channel were extended by Mg^{2+} when the $[Ca^{2+}]_i$ was relatively low. In the present study, we investigated the mechanism behind the Mg^{2+}-mediated changes in open and closed times by analyzing single-channel gating kinetics using patch clamping in the inside-out mode.

Materials and Methods

Cell Culture

Secondary cultures of RPTECs from normal human kidneys were purchased from Clonetics (Walkersville, MD). RPTECs were incubated in renal epithelial cell growth medium (REGM) (Clonetics) in a humidified atmosphere of 95% air and 5% CO_2 at 37°C. In the experiments, cells were isolated at 70 to 80% confluency after 3–6 passages with 0.025% trypsin and 0.01% EDTA and incubated on collagen-coated glass coverslips (Iwaki, Tokyo, Japan) with REGM for 3 to 10 h before use. The coverslip to which the cells adhered was then transferred into the control bath solution in a heating chamber (TC-324B, Warner, Hamden, CT). All experiments were performed at approximately 30°C, using the heating chamber.

Patch-Clamp Technique and Data Analyses

Experiments were carried out with the patch-clamp technique applied to single RPTECs, and channel recordings were performed in excised inside-out patches. Patch-clamp electrodes were made of borosilicate glass capillaries (Warner, Hamden, CT) on a two-step puller (Model PP-830, Narishige, Japan), and filled with the pipette solution described below. The electrode resistance ranged from 4 to 6 MΩ. Electric currents measured with a patch-clamp amplifier (AXOPATCH 200B, Axon, Foster City, CA) were stored on a DAT recorder (RD-120TE, TEAC, Tokyo, Japan). The current recordings were then low-pass filtered (3611 Multifunction Filter, NF, Tokyo, Japan) at 1 to 2 kHz, sampled at 10 kHz and analyzed by using the pCLAMP8 program system (Axon). Values for voltage represent the membrane potential (V_m). Currents flowing from the cytoplasmic to extracellular side were defined as outward and shown as upward deflections in figures.

Channel activity was determined by the mean channel open probability (P_o) which was calculated as

$$P_o = (1/N) \cdot \sum_{n=1}^{N} (n \cdot t_n) \quad (1)$$

where N is the number of maximally activated channels with a $[Ca^{2+}]_i$ of 10^{-3} M, n is the number of channels observed at the same time, and t_n is the probability that n channels are

simultaneously open, which was obtained by fitting the amplitude histogram with a Gaussian function of the pSTAT software included in pCLAMP 8 (Axon).

P_o and V_m data obtained from inside-out patches at each $[Ca^{2+}]_i$ were fitted by the Boltzmann curve as described below, using a least-squares regression analysis (Sohma et al., 1994).

$$P_o = P_{max} \cdot \left(1 + \exp\left[\alpha F\left(V_{1/2} - V_m\right)/RT\right]\right)^{-1} \quad (2)$$

where F, R, and T have their usual meaning, P_{max} is the maximal P_o, V_m is the membrane potential tested, $V_{1/2}$ is the membrane potential at which P_o is half-maximal, and α is the equivalent number of charges moving across the transmembrane potential during an open–close transition (the gating charge or Boltzmann constant).

The P_o and $[Ca^{2+}]_i$ data at a constant V_m obtained from inside-out patches were best fitted by the Hill equation described below.

$$P_o = P_{max}/\left[1 + \left(K_{Ca}/\left[Ca^{2+}\right]_i\right)^{N_{Ca}}\right] \quad (3)$$

where K_{Ca} and N_{Ca} are the dissociation constant and the Hill coefficient for Ca^{2+}, respectively.

The P_o and $[Mg^{2+}]_i$ data at a constant V_m obtained from inside-out patches were best fitted by the Hill equation described below.

$$P_o = P_{min} + (P_{max} - P_{min})/\left[1 + \left(K_{Mg}/\left[Mg^{2+}\right]_i\right)^{N_{Mg}}\right] \quad (4)$$

where K_{Mg} and N_{Mg} are, respectively, the dissociation constant and the Hill coefficient for Mg^{2+}, and P_{min} is the P_o at 0 mM $[Mg^{2+}]_i$.

RPTEC BK channels occasionally showed a transient unusual gating with weak activity and isolated long shut intervals, which were similar to those described by Rothberg et al. (1996). We removed these abnormal gating periods from the single-channel data used for the analysis performed in this study.

Dwell-Time Analysis for Channel Gating

To investigate the gating mechanism of RPTEC BK channels, we analyzed both one-dimensional open and closed dwell-time distributions (1-D) and two-dimensional (2-D) dwell-time distributions of sums of adjacent open-closed as well as closed-open interval pairs (*see* Rothberg, Bello & Magleby, l997, for detail). The durations of open and closed intervals were measured with a half-amplitude threshold analysis. The 1-D distributions of open and closed interval durations were log-binned at a resolution of 10 bins per log unit and plotted as the square root of the number of intervals per bin with a constant bin width on a logarithmic time axis (Sigworth & Sine, 1987). Maximum likelihood fitting with sums of exponential components was performed to estimate the time constants for 1-D open and closed dwell-time exponential components and their amplitudes using the pCLAMP8 program system (Axon). Intervals less than the dead times were excluded from the fitting.

The application of 2-D dwell-time distributions to BK channel gating analysis has been established by Magleby and his colleagues (Rothberg et al., 1997; Rothberg & Magleby, 1999, 2000). Every open interval and its subsequent (adjacent) closed interval and every closed interval and its subsequent (adjacent) open interval were combined into the 2-D dwell-time histograms, based on microscopic reversibility (Song & Magleby, 1994). The 2-D dwell-time histograms were also log-binned at a resolution of 10 bins per log unit and plotted as the normalized square root of the number of interval pairs. The interval pairs used for plotting the distribution of 2-D dwell-times were not corrected for the narrowing of intervals with a duration less than two-fold the dead time resulting from filtering. For display purposes, the 2-D surface plots were constructed from the 2-D histograms with moving bin averaging to smooth out fluctuations in the data (Rothberg & Magleby, 1998). The 2-D surface plots were generated from the smoothed data with the program MATLAB (The MathWorks, Natick, MA).

The 2-D dwell-time histograms were fitted with sums of 2-D exponential components with minimal numbers of underlying 2-D exponential components. The probability distribution function for 2-D dwell-time histograms, $pdf_{2D}(t_O, t_C)$, is defined as:

$$pdf_{2D}(t_O, t_C) = \sum_{i=1}^{N_O}\sum_{j=1}^{N_C} V_{i,j} \cdot \tau_{Oi} \cdot \tau_{Cj} \cdot \exp(-t_O/\tau_{Oi}) \cdot \exp(-t_C/\tau_{Cj}) \quad (5)$$

where N_O and N_C are the number of open and closed states, V_{ij} is the volume of each 2-D component, t_O and t_C are the open and closed times, and τ_{Oi} and τ_{Cj} are the time constants of the open and closed exponential functions.

To examine the gating mechanism based on the distribution of 2-D dwell-times, we employed a gating model (scheme I) developed by simplifying the general two-tiered gating kinetic model for a BK channel described by Rothberg & Magleby (1999, 2000). At a fixed voltage, the original two-tiered kinetic model involved five states in open and closed tiers, respectively (Rothberg & Magleby, 1999, 2000). We reduced this to two open and three closed states by omitting the states with a very low occupancy probability and/or very short mean lifetime in the experimental conditions used for the kinetic analysis (*see* Discussion).

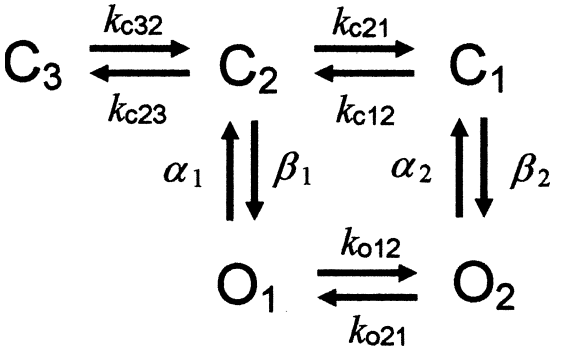

(Scheme I)

To estimate the rate constants in the gating model, we employed an iterative simulation method developed by simplifying the method described by Magleby & Weiss (1990). In brief, we developed a simulation program which, initially, generates an idealized single-channel current with no noise and an unlimited time resolution, according to the proposed gating scheme I. The idealized single-channel current was sampled at 10 kHz by adding Gaussian noise, and low-pass filtered at 2 kHz with a digital Gaussian filter (Colquhoun & Sigworth, 1995). The amplitude of the Gaussian noise was adjusted to show a root-mean-square amplitude in the final output similar to that observed in our experimental recordings. The durations of open and closed times in the simulated single-channel currents were measured with a half-amplitude threshold analysis and binned into the 2-D dwell-time histograms in a manner identical to that used to analyze the experimental data. The most likely rate constants were determined from direct likelihood comparisons of the simulated 2-D dwell-time distribution with the experimental 2-D dwell-time distribution. The fitting of data was restricted to intervals with a duration greater than two-fold the dead time. *See* Appendix 1 for more details.

All the computer programs for 2-D distribution analysis were written in FORTRAN 95 (Hewlett-Packard Company, Palo Alto, CA) and ran using the WINDOWS XP™ operating system (Microsoft, Redmond, WA) on a personal computer fitted with an Intel Pentium 4™ processor (Dell, Round Rock, TX).

Solutions

The pipette solution for inside-out patches contained (mM): 145 KCl, 3 $MgCl_2$, 1 EGTA, and 5 HEPES, pH 7.3. The control bath solution contained (mM): 140 NaCl, 5 KCl, 1 $MgCl_2$, 1 $CaCl_2$, 5 glucose, and 5 HEPES, pH 7.3. Experimental bath solutions contained (mM): 145 KCl, 0–10 $MgCl_2$, and 5 HEPES with 10^{-6}–10^{-3} M free Ca^{2+}. The solutions with 10^{-5}–10^{-3} M free Ca^{2+} were prepared by adding $CaCl_2$ without EGTA. The solutions with $10^{-5.5}$ and 10^{-6} M free Ca^{2+} were adjusted by the addition of an adequate amount of $CaCl_2$ and EGTA (10 mM) according to the computer program of Oiki & Okada (1987), which was made by using the absolute values of the stability constant of EGTA for the binding of Ca^{2+}, Mg^{2+}, and H^+ (Martell & Smith, 1977). Experimental bath solutions with a pH adjusted to 7.3 were made by adding HCl or KOH. The free Ca^{2+} concentration and pH of all solutions were checked simultaneously with a Ca^{2+}-electrode (CL-125B, TOA, Tokyo, Japan) and a pH-electrode (GST-5311C, TOA), respectively, at approximately 30°C.

Statistics

Data are expressed as means ± SE. Statistical significance was determined by using the Student *t* -test or ANOVA in conjunction with the Tukey *t*-test (Curran-Everett, 2000). A *P* value of less than 0.05 was considered significant.

Results

Effects of $[Mg^{2+}]_i$ and V_m on Single-Channel Current of The BK Channel in RPTECs

Figure 1*A* shows current recordings of a BK channel in RPTECs in response to V_m at 0 or 10 mM Mg^{2+} and 10^{-4} M Ca^{2+}. It is apparent that P_o was markedly altered by changes in V_m at a constant $[Mg^{2+}]_i$, whereas adding 10 mM Mg^{2+} at a constant V_m reduced current amplitude dose-dependently with a moderate elevation of P_o. Raising the $[Mg^{2+}]_i$ from 0 to 10 mM increased P_o from 0.17 to 0.80 at a V_m of −60 mV in the lower traces, although the increase induced by adding 10 mM Mg^{2+} was only slight when P_o was nearly maximum even in the absence of Mg^{2+}, as shown in the upper traces. In addition, the blocking effect of internal Mg^{2+} on current amplitude is stronger at a positive than a negative V_m.

The current-voltage (*I–V*) relationship under similar conditions as shown in Fig. 1*A* is illustrated in Fig. 1*B*. In the absence of Mg^{2+}, the *I–V* relationship was almost linear at 10^{-4} M Ca^{2+}, and the slope conductance was 322.6 ± 2.3 pS (n = 4). Adding Mg^{2+} at 1, 3 or 10 mM suppressed the current amplitude, particularly at a positive V_m. The suppression of current amplitude became greater as the $[Mg^{2+}]_i$ increased and as the V_m was made more positive. Thus the Mg^{2+}-induced suppression was suggested to be dependent on both $[Mg^{2+}]_i$ and V_m (Fig. 1), which was similar to the results obtained for BK channels in cells other than RPTECs (Tabcharani & Misler, 1989; Ferguson, 1991; Zhang et al., 1995; Morales et al., 1996; Wachter & Turnheim, 1996; Bringmann et al., 1997; Kazachenko & Chemeris, 1998).

Effects of Mg^{2+} on the P_o–V_m Relationship at Various Concentrations of Ca^{2+}

Since Mg^{2+} and V_m affected channel P_o, as shown in Fig. 1*A*, we tested the effects of raising $[Mg^{2+}]_i$ on the P_o–V_m relationship at various concentrations of Ca^{2+}. Figure 2*A–D* represents P_o–V_m relationships at 0, 1, 3 and 10 mM $[Mg^{2+}]_i$ with a $[Ca^{2+}]_i$ of 10^{-4}, 10^{-5}, $10^{-5.5}$ and 10^{-6} M at a V_m ranging from −75 to 75 mV. The P_o data were best fitted with the Boltzmann equation (Eq. 2). Raising the $[Mg^{2+}]_i$ shifted the P_o–V_m relationship to the left on the voltage axis at 10^{-4}–10^{-5} M Ca^{2+}. These results indicate that raising the $[Mg^{2+}]_i$ increases P_o of the BK channel. However, the Mg^{2+}-induced shift in the P_o–V_m relationship was markedly suppressed at $10^{-5.5}$ and 10^{-6} M Ca^{2+}, suggesting that Mg^{2+} required a relatively high $[Ca^{2+}]_i$ to increase P_o.

The voltages of half-maximum activation ($V_{1/2}$) obtained from P_o–V_m relationships (Fig. 2) are shown in Fig. 3*A*. Although $[Mg^{2+}]_i$ was scaled logarithmically on the abscissa, data at 0 mM Mg^{2+} are represented to compare the data of Ca^{2+} alone in the presence of Mg^{2+}. The values of $V_{1/2}$ at 0 mM Mg^{2+} in the presence of 10^{-4}, 10^{-5}, $10^{-5.5}$, and 10^{-6} M Ca^{2+} were −32.2, 5.6, 27.7 and 59.5 mV, respectively. Raising the $[Mg^{2+}]_i$ to 10 mM shifted the $V_{1/2}$ to −86.2 mV at a $[Ca^{2+}]_i$ of 10^{-4} M, to −33.3 mV at 10^{-5} M, to 19.6 mV at $10^{-5.5}$ M, and to 55.6 mV at 10^{-6} M. The changes in $V_{1/2}$ caused by adding 10 mM Mg^{2+} at 10^{-4}, 10^{-5}, $10^{-5.5}$ and 10^{-6} M Ca^{2+} were −53.9, −27.7, −8.1 and −3.9 mV, indicating that lowering the $[Ca^{2+}]_i$ decreases the Mg^{2+}-induced shift in the P_o–V_m relationship, as was shown in Fig. 2. Fig. 3*B* shows values of the gating charge (α) obtained from the data on P_o–V_m relationships, in Fig. 2*A–D*. These data indicate that the values of α were not significantly altered by changes in $[Mg^{2+}]_i$ at any $[Ca^{2+}]_i$ adopted in this study, suggesting that the Mg^{2+}-mediated shift of the P_o–V_m relationship (Fig. 2) was not due to alteration of the sensitivity to voltage.

Mutual Effects of $[Mg^{2+}]_i$ and $[Ca^{2+}]_i$ on P_o of The BK Channel

Figure 4*A* represents the P_o–$[Ca^{2+}]_i$ relationships fitted using Eq. 3 at 0 (*filled circles*), 1 (*filled squares*), 3 (*filled triangles*) and 10 mM (*filled diamonds*) Mg^{2+}

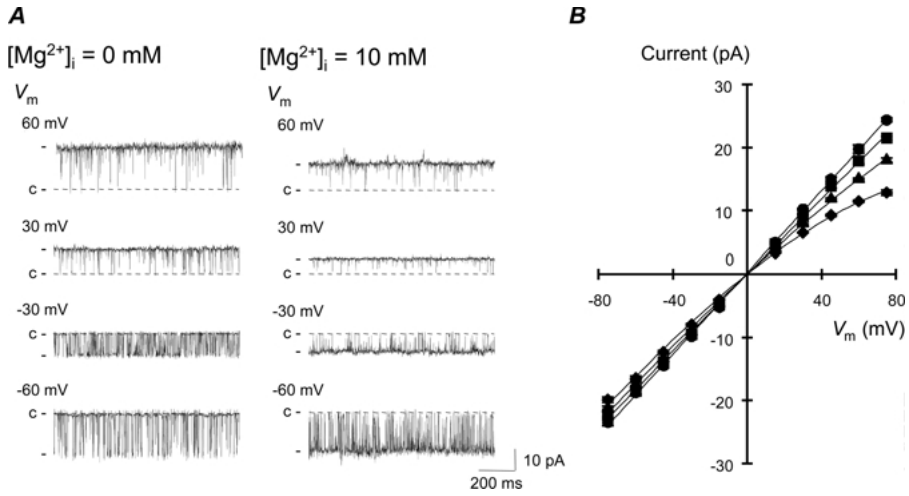

Fig. 1. Effects of $[Mg^{2+}]_i$ and V_m on single-BK-channel currents of RPTECs at a constant $[Ca^{2+}]_i$. (*A*) Single-channel recordings of a BK channel observed with $[Mg^{2+}]_i$ of 0 and 10 mM at a V_m of 60, 30, −30 and −60 mV in an inside-out patch under a symmetrical 145 mM KCl solution with a $[Ca^{2+}]_i$ of 10^{-4} M. The traces were filtered at 1 kHz and digitized at 10 kHz. The values for the respective $[Mg^{2+}]_i$ are indicated atop the traces, and those for V_m in mV are indicated atop each trace. The current levels of the channel are indicated by short bars (left), and closed channels are indicated by dotted lines and "*C*". (*B*) Current-voltage (*I–V*) relationships of the BK channels with 0 mM (●), 1 mM (■), 3 mM (▲) and 10 mM (♦) Mg^{2+} in inside-out patches ($n = 4$). The pipette and bath solutions used were the same as described above. The *I–V* relationship at 0 mM Mg^{2+} was fitted by a straight line, and others were fitted by the equation: $i_o / i_{Mg} = 1 + ([Mg^{2+}]_i / K_{d0} \exp(z\delta V_m F / RT)$, where i_o / i_{Mg} is the ratio of the current in the absence and the presence of Mg^{2+}, K_{d0} is the dissociation constant of Mg^{2+} at 0 mV, and $z\delta$ is the effective valence of the Mg^{2+} block (Woodhull, 1973; Ferguson, 1991).

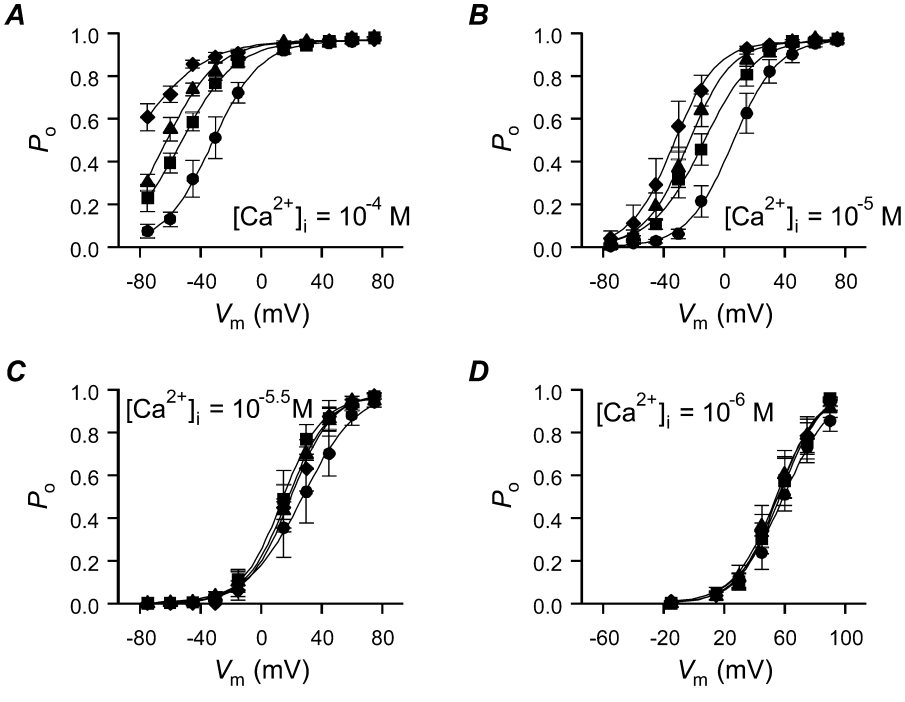

Fig. 2. Effects of $[Mg^{2+}]_i$ on P_o–V_m relationships of the BK channels in inside-out patches. P_o–V_m relationships at a bath $[Ca^{2+}]_i$ of 10^{-4} M (*A*), 10^{-5} M (*B*), $10^{-5.5}$ M (*C*), and 10^{-6} M (*D*) in symmetrical 145 mM KCl solutions. The bath solutions with Ca^{2+} contained 0 mM (●), 1 mM (■), 3 mM (▲) and 10 mM (♦) Mg^{2+}. The lines were fitted by Eq. 2. Data from 6 patches.

and a V_m of −45 mV. This V_m resulted in a marked difference in P_o induced by changes in $[Ca^{2+}]_i$ and $[Mg^{2+}]_i$. The K_{Ca} (M) at 0, 1, 3 and 10 mM $[Mg^{2+}]_i$ was $10^{-3.51}$, $10^{-4.33}$, $10^{-4.70}$ and $10^{-4.87}$, respectively, indicating that raising the $[Mg^{2+}]_i$ shifts the P_o–$[Ca^{2+}]_i$ relationship to a lower $[Ca^{2+}]_i$. Furthermore, the Hill coefficient (N_{Ca}) at 0, 1, 3 and 10 mM $[Mg^{2+}]$ was 0.73, 1.11, 1.70 and 2.51, respectively. Taken together, raising the $[Mg^{2+}]_i$ results in an enhancement of the sigmoidicity of the P_o–$[Ca^{2+}]_i$ relationship. Therefore, it appears that raising the $[Mg^{2+}]_i$ changes the sensitivity to Ca^{+} and increases the

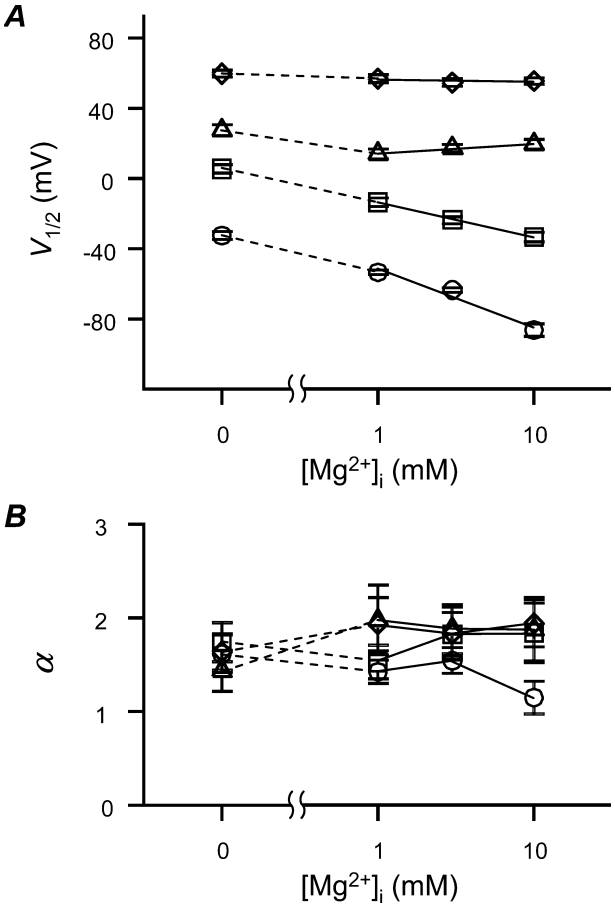

Fig. 3. Effects of $[Mg^{2+}]_i$ on voltage-sensitivity of the BK channels. (*A*) The plots of $V_{1/2}$ against $[Mg^{2+}]_i$ were obtained from individual relationships in Fig. 2. Data were determined using bath solutions with four different $[Ca^{2+}]_i$ (○, 10^{-4} M; □, 10^{-5} M; Δ, $10^{-5.5}$ M; ◇, 10^{-6} M). The lines were fitted by straight lines. (*B*) These plots of α against $[Mg^{2+}]_i$ were obtained from individual relationships in Fig. 2. Data were determined using bath solutions with four different $[Ca^{2+}]_i$ (○, 10^{-4} M; □, 10^{-5} M; Δ, $10^{-5.5}$ M; ◇, 10^{-6} M).

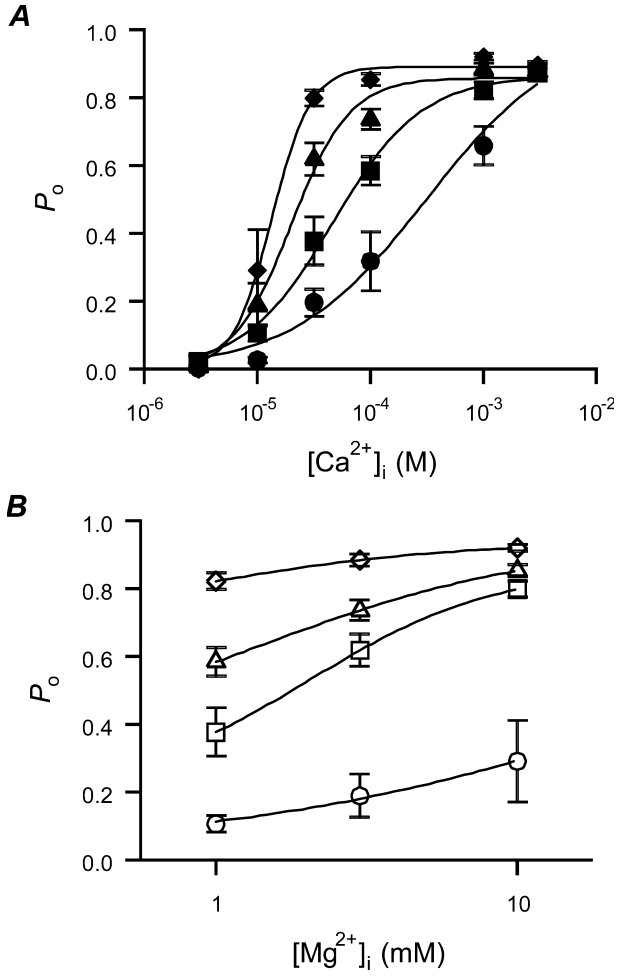

Fig. 4. Relationship between P_o and $[Ca^{2+}]_i$ or $[Mg^{2+}]_i$ of the BK channels at a constant V_m. (*A*) Relationship between P_o and $[Ca^{2+}]_i$ in conditions with a $[Mg^{2+}]_i$ of 0 mM (●), 1 mM (■), 3 mM (▲) and 10 mM (♦) in inside-out patches. These plots were adopted from the data obtained at a V_m of −45 mV in Fig.2. Values of P_o under conditions where the $[Ca^{2+}]$ is of 10^{-3} and $10^{-2.5}$ M, $[Mg^{2+}]_i$ is 0–10 mM, and V_m is −45 mV were also plotted to clarify this relationship in detail. The lines were best fitted by Eq. 3. (*B*) Relationship between P_o and $[Mg^{2+}]_i$ in the presence of a $[Ca^{2+}]_i$ of 10^{-5} M (○),$10^{-4.5}$ M (□), 10^{-4} M (Δ) and 10^{-3} M (◇) in inside-out patches. The data used are the same as those represented in Fig. 4*A*. The lines were best fitted by Eq. 4.

apparent cooperativity of Ca^{2+} in activating the channel.

Figure 4*B* shows the P_o–$[Mg^{2+}]_i$ relationships depicted using the same data as adopted in Fig. 4*A*. The lines were fitted by Eq. 4 at 10^{-5}, $10^{-4.5}$, 10^{-4} and 10^{-3} M Ca^{2+}. The data obtained at $10^{-5.5}$ and 10^{-6} M Ca^{2+} were excluded, since P_o at this concentration was very low even in the presence of Mg^{2+}. The K_{Mg} at $10^{-4.5}$, 10^{-4} and 10^{-3} M $Ca^{2+}$was 2.04, 1.37 and 0.72 mM, respectively, indicating that raising the $[Ca^{2+}]_i$ decreased the dissociation constant for Mg^{2+}. The Hill coefficient for Mg^{2+} (N_{Mg}) at $10^{-4.5}$, 10^{-4} and 10^{-3} M $Ca^{2+}$was 1.39, 0.92 and 1.00, respectively. The value of N_{Mg} was not markedly altered by increasing the $[Ca^{2+}]_i$, suggesting that Ca^{2+}-mediated channel activation was not significantly affected by Mg^{2+} at a concentration of Ca^{2+} higher than $10^{-4.5}$ M.

Therefore, the simplest interpretation of these results is that the Mg^{2+}-mediated enhancement of P_o in this BK channel would result from increases in sensitivity to Ca^{2+} under the conditions adopted in this experiment, which is consistent with the "via Ca^{2+}-sensitivity" scheme proposed by Golowasch et al., (1986) and Oberhauser et al., (1988).

Effects of $[Mg^{2+}]_i$ and $[Ca^{2+}]_i$ on Mean Dwell-Time of the BK Channels

To further examine whether the Mg^{2+}-induced increase in P_o resulted from an alteration of the sensitivity of the channel to Ca^{2+}, we attempted to

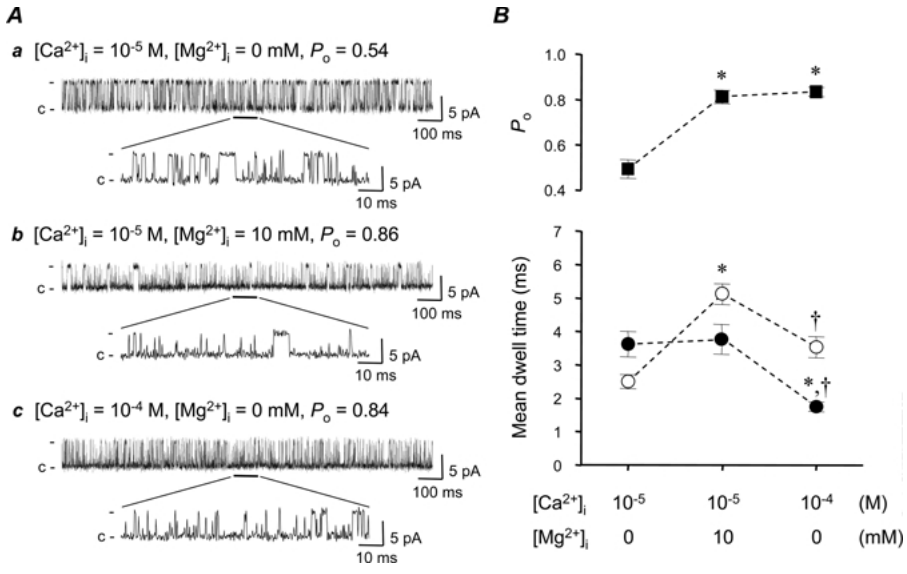

Fig. 5. Effects of raising the $[Mg^{2+}]_i$ or $[Ca^{2+}]_i$ on the gating of the BK channels. (*A*) Single channel recordings of a BK channel in response to the raising of the $[Mg^{2+}]_i$ or $[Ca^{2+}]_i$ in an inside-out patch. The pipette solution contained 145 mM KCl. The bath solutions used were 145 mM KCl containing the $[Ca^{2+}]_i$ or $[Mg^{2+}]_i$ represented on the top of each trace. Data were obtained from channel recordings filtered at 2 kHz and digitized at 10 kHz with the V_m held at −15 mV The current of the channel is indicated by short bars (left), and closed channels are indicated by "*C*". (B) Summarized data on effects of increasing the $[Mg^{2+}]_i$ or $[Ca^{2+}]_i$ on P_o and the mean dwell time of the BK channels in inside-out patches. P_o (■), mean open time (○), and mean closed time (●) were obtained from single channel recordings at V_m of −15 mV ($n = 6$) at the various $[Ca^{2+}]_i$ and $[Mg^{2+}]_i$ indicated on the abscissa. *Significantly different ($P < 0.05$) from values obtained in the presence of 10^{-5} M Ca^{2+} and the absence of Mg^{2+}. †Significantly different ($P < 0.05$) from values obtained in the presence of 10^{-5} M Ca^{2+} and 10 mM Mg^{2+}.

characterize the Mg^{2+}-mediated channel gating using the mean dwell-time obtained from single BK channels. Figure 5*A* shows changes in channel currents in response to 10 mM Mg^{2+} added in the presence of 10^{-5} M Ca^{2+} and to raising the $[Ca^{2+}]_i$ from 10^{-5} to 10^{-4} M. Compared with the channel current observed in the absence of Mg^{2+} at 10^{-5} M Ca^{2+} (*upper trace*), addition of 10 mM Mg^{2+} markedly extended the open time (*middle trace*), whereas raising the $[Ca^{2+}]_i$ to 10^{-4} M in the absence of Mg^{2+} shortened the long closed time (*lower trace*).

Figure 5*B* summarizes data on P_o (*filled square*), mean open time (*empty circle*) and mean closed time (*filled circle*) of single channels ($n = 5$) under similar conditions as shown in Fig. 5*A*. P_o in the absence of Mg^{2+} at 10^{-5} M Ca^{2+} (*control*), in the presence of 10 mM Mg^{2+} at 10^{-5} M Ca^{2+} (*high Mg^{2+}*) and in the absence of Mg^{2+} at 10^{-4} M Ca^{2+} (*high Ca^{2+}*) was 0.49 ± 0.04, 0.81 ± 0.03 and 0.83 ± 0.02, respectively. Mean open times (ms) in the control, high Mg^{2+} and high Ca^{2+} groups were 2.50 ± 0.21, 5.24 ± 0.31 and 3.53 ± 0.32, whereas mean closed times (ms) were 3.62 ± 0.38, 3.62 ± 0.45 and 1.75 ± 0.15, respectively. Note that P_o in the high Mg^{2+} group was similar to that in the high Ca^{2+} group despite the differences in mean dwell times between the two groups. Although a similar elevation of P_o was unexpectedly obtained, these data indicate that addition of 10 mM Mg^{2+} at a constant $[Ca^{2+}]_i$ increases P_o by markedly extending the mean open time, whereas raising the $[Ca^{2+}]_i$ from 10^{-5} to 10^{-4} M at a constant $[Mg^{2+}]_i$ increases P_o by mainly shortening the mean closed time.

Figure 6 shows effects of raising the $[Mg^{2+}]_i$ or $[Ca^{2+}]_i$ on the distribution of open and closed times. The distribution of open and closed times is fitted by two (τ_{O1} and τ_{O2}) and three (τ_{C1}, τ_{C2} and τ_{C3}) exponential components, respectively (Fig. 6*A*). Neither raising the $[Mg^{2+}]_i$ from 0 to 10 mM at a constant $[Ca^{2+}]_i$ (Fig. 6*A-ab*) nor raising the $[Ca^{2+}]$i from 10^{-5} to 10^{-4} M with 0 mM Mg^{2+} (Fig. 6*C-ab*) significantly affected the time constants of open and closed times except for a slight (~1.6-fold) increase in the time constants of the open distribution. In terms of the proportion of each component, raising both the $[Mg^{2+}]_i$ and $[Ca^{2+}]_i$ increased the proportion of the fastest τ_{C1} component and decreased the proportion of the moderate τ_{C2} component in closed time distributions (Fig. 6*B-d* and 6*C-d*). However, a predominant difference between Mg^{2+} and Ca^{2+} is found in the proportion of their open-time components (Fig. 6*B-c* and 6*C-g*), that is, raising the $[Mg^{2+}]_i$ increased the proportion of the slower τ_{O2} component from 0.12 to 0.53 and decreased the proportion of the faster τ_{O1} component from 0.88 to 0.47 (Figs. 6B-*c*),whereas raising the $[Ca^{2+}]_i$ did not have a significant effect (Fig. 6*C-c*).

Thus the different effects of raising the $[Mg^{2+}]_i$ and $[Ca^{2+}]_i$ on channel gating suggested that the

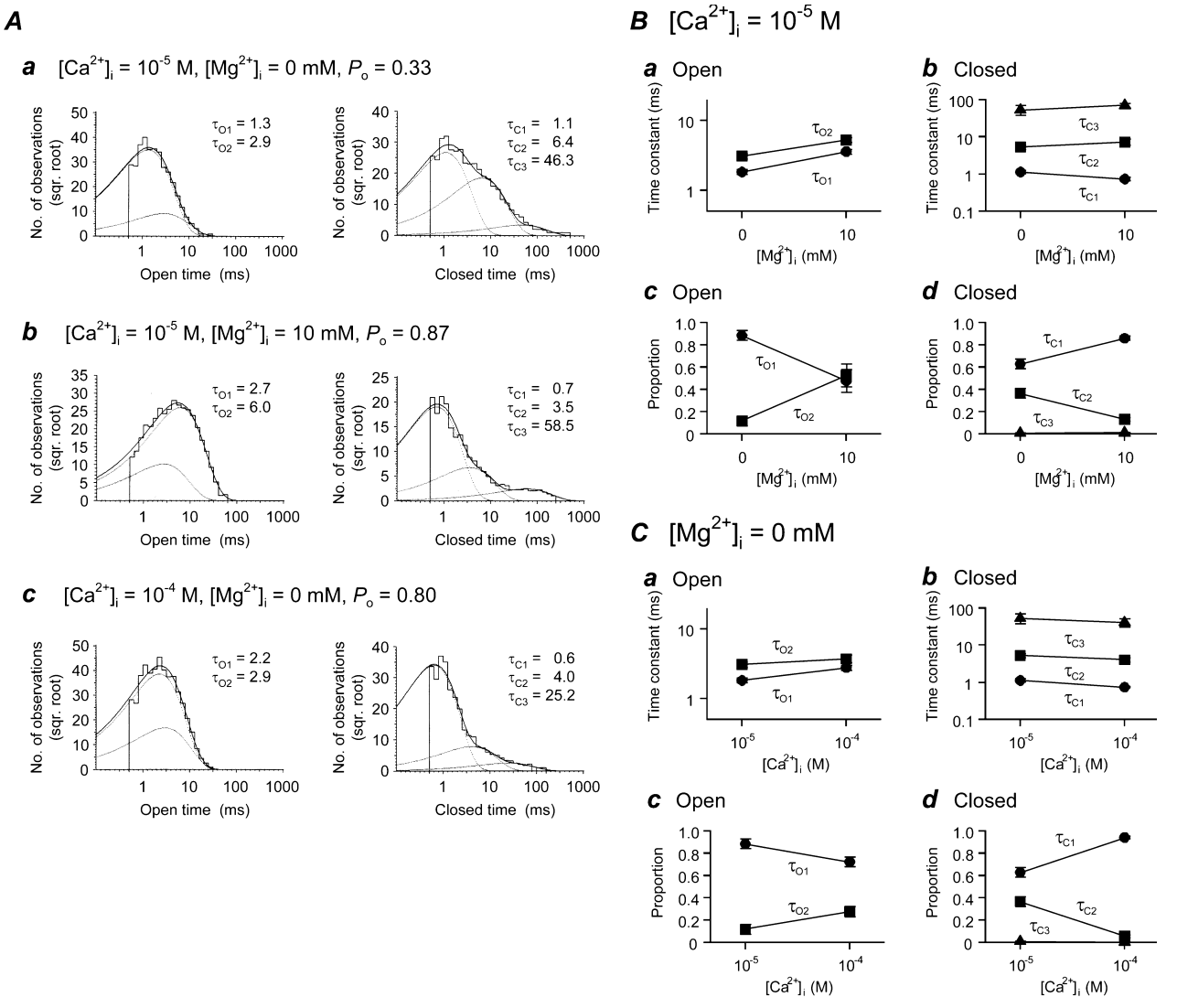

Fig. 6. Changes in open and closed dwell-time distributions in response to raising the $[Mg^{2+}]_i$ or $[Ca^{2+}]_i$. (*A*) Open and closed 1-D dwell-time histograms obtained from a single channel recording at (*a*) 10^{-5} M Ca^{2+} with 0 Mg^{2+}, (*b*) 10^{-5} M Ca^{2+} with 10 mM Mg^{2+}, and (*c*) 10^{-4} M Ca^{2+} with 0 Mg^{2+}. The open and closed times were plotted on the abscissa with a logarithmic scale, and the square root of the number of observations was plotted on the ordinate. The open-time histograms were best fitted by the sum of two, (τ_{O1} and τ_{O2} ($\tau_{O1} < \tau_{O2}$), exponential components, and closed time histograms by the sum of three, τ_{C1}, τ_{C2} and τ_{C3} ($\tau_{C1} < \tau_{C2} < \tau_{C3}$), exponential components, using the maximum likelihood fitting method. $V_m = -15$ mV. (*B*) Effects of $[Mg^{2+}]_i$ on time constants of (*a*) open and (*b*) closed 1-D dwell-time distributions and proportion of each exponential component in (*c*) open and (*d*) closed 1-D dwell-time distributions at a constant $[Ca^{2+}]_i$ of 10^{-5} M ($n = 5$). (*C*) Effects of $[Ca^{2+}]_i$ on time constants of (*a*) open and (*b*) closed 1-D dwell-time distributions and proportion of each exponential component in (*c*) open and (*d*) closed 1-D dwell-time distributions with 0 mM $[Mg^{2+}]$; ($n = 5$).

mechanism for channel activation induced by raising the $[Mg^{2+}]_i$ would be different from that induced by raising the $[Ca^{2+}]_i$. This finding is inconsistent with the classical "via Ca^{2+}" scheme (Golowasch et al., 1986; Oberhauser et al., 1988).

Effects of $[Ca^{2+}]_i$ or V_m on The Relationship between K_{Mg} And P_{min}

The major action of internal Mg^{2+} on the activity of the BK channel was suggested to be to extend the time of the channel opening as mentioned above, which was considered different from $[Ca^{2+}]_i$- or V_m-mediated changes in channel activity. Thus, next we examined whether the Mg^{2+}-mediated enhancement of P_o resulted solely from the lengthening of the open time or partially from a change in sensitivity to $[Ca^{2+}]_i$ or V_m For this purpose, relationships between K_{Mg} and P_{min} (P_o with 0 mM $[Mg^{2+}]_i$, *see* Eq. 4) were plotted and compared at different concentrations of Ca^{2+} or V_m values.

Figure *7A* shows the log-log plots of K_{Mg} against P_{min} at various V_m values with 10^{-5} and 10^{-4} M Ca^{2+}. Values of P_{max} with 10^{-5} M Ca^{2+} (*filled squares*) were

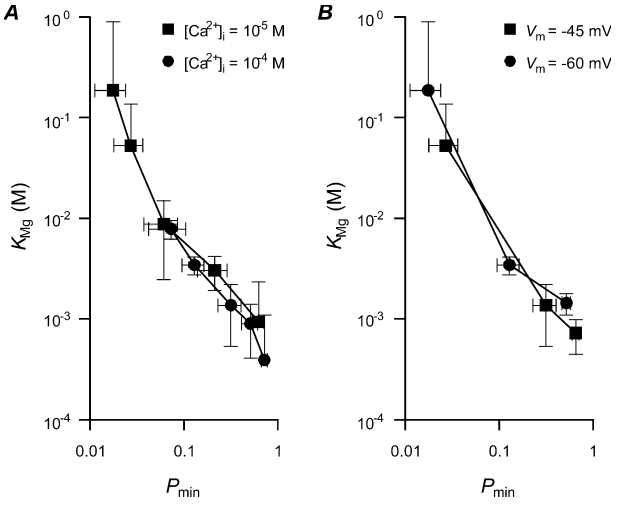

Fig. 7. Relationship between K_{Mg} and P_{min} of the BK channel under conditions with a different $[Ca^{2+}]_i$ or V_m. (*A*) Relationship between K_{Mg} and P_{min} at 10^{-5} and 10^{-4} M Ca^{2+} in inside-out patches. K_{Mg} is the dissociation constant for Mg^{2+} and P_{min} is P_o at 0 mM $[Mg^{2+}]_i$-P_{min} values at 10^{-5} M Ca^{2+} (■) were obtained at a V_m of −60, −45, −30 and −15 mV, and those at 10^{-4} M Ca^{2+} (●) were obtained with a V_m of −75, −60, −45, −30 and −15 mV, respectively. K_{Mg} values were obtained from P_o–$[Mg^{2+}]_i$ relationships fitted by Eq. 4. (*B*) Relationship between K_{Mg} and P_{min} at a V_m of −60 and −45 mV in inside-out patches. Individual values for P_{min} at −45 mV (■) and −60 mV (●) were obtained from conditions with 10^{-5}, 10^{-4} and 10^{-3} M $[Ca^{2+}]_i$, respectively). K_{Mg} was obtained from the P_o–$[Mg^{2+}]_i$ relationship fitted by Eq. 4.

obtained at a V_m of −60, −45, −30 and −15 mV, and those with 10^{-4} M Ca^{2+} (*filled circles*) were obtained at a V_m of −75, −60, −45, −30 and −15 mV. The K_{Mg} values were obtained from P_o–$[Mg^{2+}]_i$ relationships fitted using Eq. 4. K_{Mg} is strongly dependent on P_{min} and the K_{Mg}–P_{min} relationships show a slope close to −1 in the log-log plots. Although P_{min} values differed in the series of 10^{-5} and 10^{-4} M Ca^{2+} experiments, the K_{Mg}–P_{min} relationships overlapped, suggesting that K_{Mg} was independent of the $[Ca^{2+}]_i$ of 10^{-5} and 10^{-4} M, but dependent on P_{min}. The fact that the slope of the K_{Mg}–P_{min} relationships is close to −1 suggests that Mg^{2+} binds to the BK channel only in its open conformation (*see* Appendix 2).

The K_{Mg}–P_{min} relationships at various concentrations of Ca^{2+} and a V_m of −45 and −60 mV are represented in Fig. 7*B*. Individual values for P_{min} at −45 mV (*filled squares*) and −60 mV (*filled circles*) were obtained from the conditions with 10^{-5}, 10^{-4} and 10^{-3} M Ca^{2+}, respectively. The K_{Mg}–P_{min} relationships at V_ms of −45 and −60 mV also overlapped with a slope close to −1, suggesting that K_{Mg} was independent of V_m but dependent on P_{min} according to the open-channel binding scheme (*see* Appendix 2).

Taken together, these results strongly suggest that the Mg^{2+}-induced enhancement of P_o is solely dependent on the basal P_o before the addition of Mg^{2+}, and independent of $[Ca^{2+}]_i$ or V_m in the range adopted in this analysis. Moreover, the binding of Mg^{2+} to the BK channel is suggested to occur only in its open conformation.

Effects of High $[Mg^{2+}]_i$ on P_o and Mean Dwell-Time at a Relatively Low $[Ca^{2+}]_i$

As shown in Fig. 2C and *D*, P_o–V_m relationships at $10^{-5.5}$ and 10^{-6} M Ca^{2+} were not significantly affected by raising the $[Mg^{2+}]_i$. These results indicate that Mg^{2+}-mediated enhancement of P_o was suppressed at such relatively low concentrations of Ca^{2+}. Therefore, we further examined the effect of adding 10 mM Mg^{2+} on the mean dwell times of the BK channel at $10^{-5.5}$ M Ca^{2+} to clarify why the effect of Mg^{2+} was diminished at this relatively low $[Ca^{2+}]_i$. Figure 8*A* shows actual recordings of a single BK channel at a V_m of 15 mV in the presence of $10^{-5.5}$ M Ca^{2+} before (Fig.8*A-a*) and after (Fig.8*A-b*) 10 mM Mg^{2+} was added. The channel currents mainly consisted of short open periods with a P_o of 0.28 in the presence of $10^{-5.5}$ M Ca^{2+} alone, which was remarkably changed by 10 mM Mg^{2+}. Namely, adding 10 mM Mg^{2+} extended both the open and closed times of the channel with suppression of the current amplitude. The suppression of the current amplitude was similar to that represented in Fig. 1. Furthermore, it is possible that the Mg^{2+} contains a small amount of Ba^{2+}, which may cause the long closed time (Neyton, 1995). However, the concentration of Ba^{2+} in the 10 mM Mg^{2+} solutions was less than 0.2 μM, which had little inhibitory effect on the BK channels in RPTECs at a V_m of 15 mV (*data not shown*).

Figure 8*B* summarizes the data on P_o (*filled squares*), the mean open time (*empty circles*) and the mean closed time (*filled circles*) obtained from 4 single channels. Adding 10 mM Mg^{2+} failed to increase P_o significantly (from 0.35 ± 0.12 to 0.41 ± 0.11), whereas it significantly increased both the mean open time (from 3.87 ± 0.30 and 7.07 ± 1.25 ms) and the mean closed time (from 20.05 ± 11.22 to 30.73 ± 6.82 ms).

Figure 9 shows the distribution of open and closed dwell-times in a single BK channel at $10^{-5.5}$ M Ca^{2+}. Even at this $[Ca^{2+}]_i$, the distribution of open and closed times is well-fitted by two and three exponential components, respectively, at both 0 and 10 mM $[Mg^{2+}]i$ (Fig. 9*A*). In the open time distribution, raising the $[Mg^{2+}]_i$ from 0 to 10 mM at a constant $[Ca^{2+}]_i$ of $10^{-5.5}$ M increased τ_{O1} and τ_{O2} (Fig.9*B-a*) and decreased the proportion of the τ_{O1} component and increased that of the τ_{O2} component significantly (Fig.9*B-c*). The addition of Mg^{2+} also decreased the proportion of the τ_{C2} component and increased that of the τ_{C1} component (Fig. 9*B-b*) with

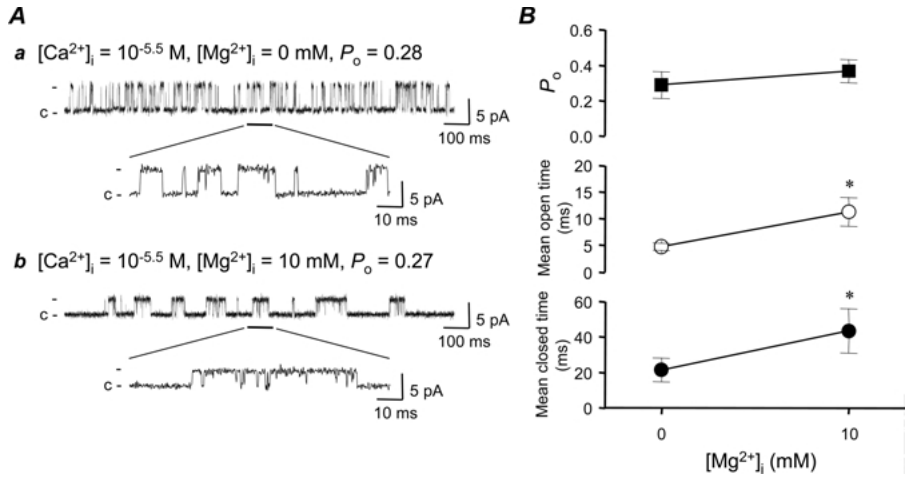

Fig. 8. Effects of raising $[Mg^{2+}]_i$ on the gating of BK channels at a relatively low $[Ca^{2+}]_i$ ($10^{-5.5}$ M). (*A*) Actual recordings of a single BK channel at a V_m of 15 mV in the presence of $10^{-5.5}$ M Ca^{2+} (*a*) before and (*b*) after adding 10 mM Mg^{2+}. The channel P_o before and after addition of 10 mM Mg^{2+} in the presence of $10^{-5\ 5}$ M Ca^{2+} was 0.28 and 0.27, respectively. (*B*) Summarized data on changes in P_o (■), mean open time (○) and mean closed time (●) before and after 10 mM Mg^{2+} was added in the presence of $10^{-5.5}$ M Ca^{2+} at a V_m of 15 mV. The data were obtained from 6 single BK channels. *Significantly different ($P < 0.05$) from the value before 10 mM Mg^{2+} was added.

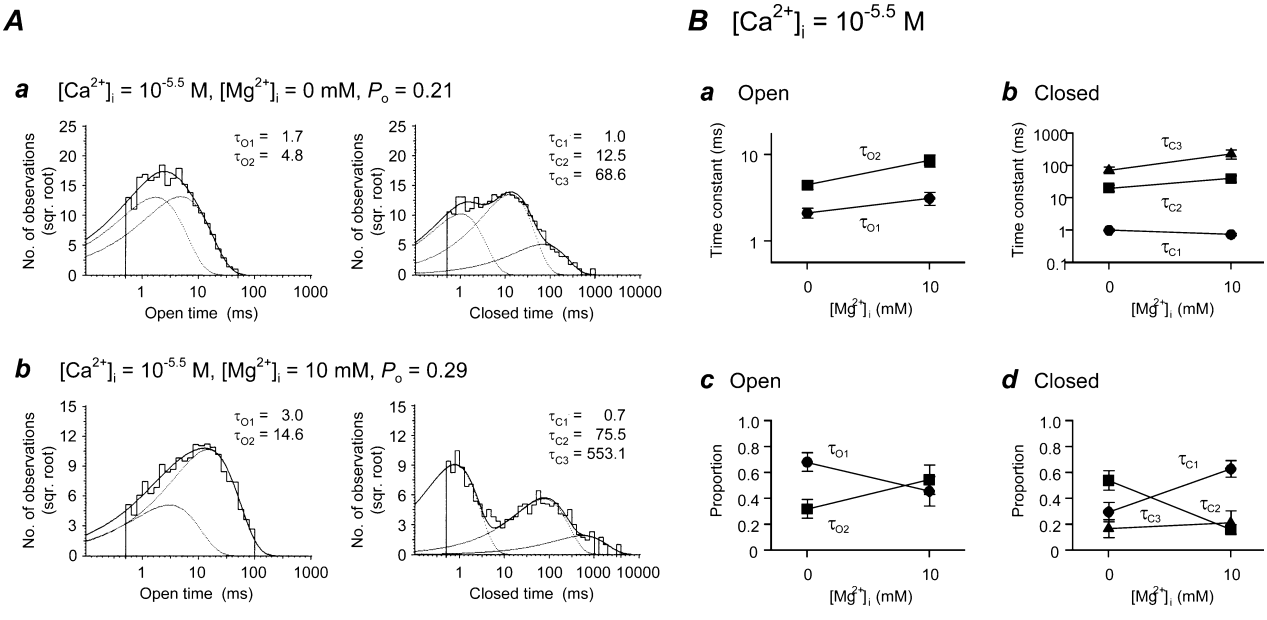

Fig. 9. Effects of raising $[Mg^{2+}]_i$ on open and closed dwell-time distributions at a relatively low $[Ca^{2+}]$j. (*A*) Open and closed 1-D dwell-time histograms obtained from a single-channel recording at $10^{-5.5}$ M Ca^{2+} (*a*) before and (*b*) after 10 mM Mg^{2+} was added at a V_m of 15 mV. *(B)* Effects of $[Mg^{2+}]_i$ on time constants of (*a*) open and (*b*) closed 1-D dwell-time distributions and proportion of each exponential component in (*c*) open and (*d*) closed dwell-time distributions at a constant $[Ca^{2+}]_i$ of $10^{-5\ 5}$ M ($n = 4$).

increasing τ_{C2} and τ_{C3} (Fig. 9*B-d*). The open time would be extended by increasing the $[Mg^{2+}]_i$ as indicated above, however, a simultaneous lengthening of the closed time should result in a suppression of the increase in P_o.

The extension of the closed time might be due to interference from the high concentration of Mg^{2+} with Ca^{2+}-binding to the sites in which Ca^{2+} enhances channel activity, since Ca^{2+}-induced changes in channel activity mainly result from alterations of the closed time as shown in Fig. 5. Thus, it is plausible that the lengthening of the open time of the BK channel caused by adding Mg^{2+} does not result from changes in sensitivity to Ca^{2+}, whereas that of the closed time caused by a high $[Mg^{2+}]_i$ at a relatively low $[Ca^{2+}]_i$ may be induced by competitive inhibition

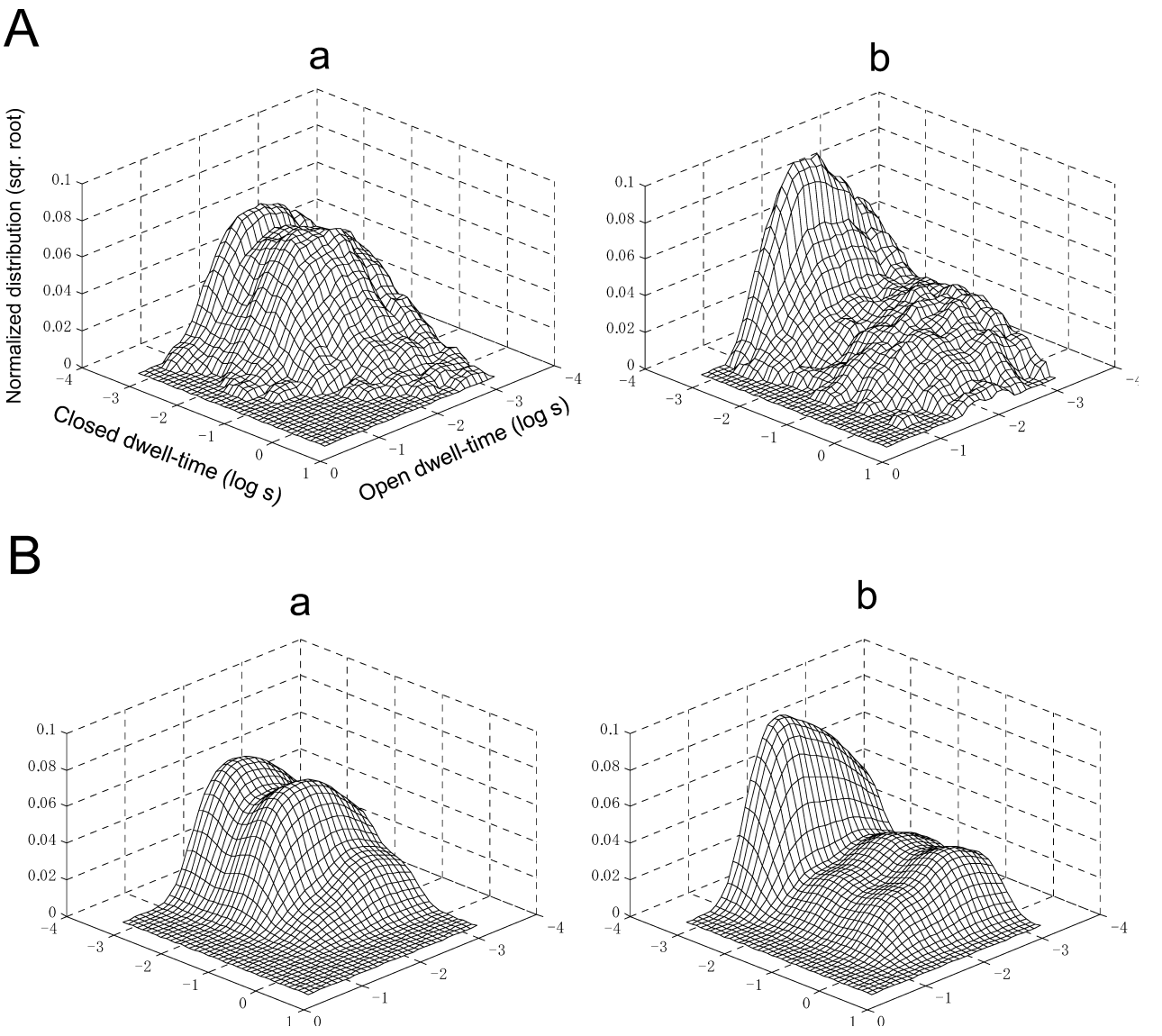

Fig. 10. Two-dimentional analysis of the effects of Mg^{2+} on RPTEC BK channel gating (I) (*A*). 2-D dwell-time distribution of adjacent open and closed intervals of experimental data with (*a*) 0 mM and (*b*) 10 mM Mg^{2+}. Adjacent open and closed intervals were binned as pairs, with the log of the open and closed interval durations on the *x* and *y* axes, respectively. The *z* axis plots the square root of the number of intervals in each bin. The data are plotted for binning at a resolution of 10 bins per log unit. (*B*) Sums of two open and three closed 2-D components best-fitted to the experimental 2-D dwell-time distribution with (*a*) 0 mM and (*b*) 10 mM Mg^{2+} shown in Fig. 10*A*. Parameters are shown in Table 1.

of the binding of Ca^{2+} to its affinity site by Mg^{2+}, which could cause the change in the Hill coefficient as shown in Fig. 4A.

A Model of The Gating of BK Channels in Response to Mg^{2+} and Ca^{2+}

Finally, using the 2-D dwell-time distribution analysis, we investigated the effects of Mg^{2+} on the gating of RPTEC BK channels at a low $[Ca^{2+}]_i$ in more detail. Figures 10*A-a* and *b* show 2-D dwell-time histograms of adjacent open-closed and closed-open interval pairs obtained from a single channel at 0 and 10 mM Mg^{2+} at $10^{-5.5}$ M Ca^{2+}. The application of 10 mM Mg^{2+} induced a drastic change in the distribution of the 2-D dwell-time of the RPTEC BK channels (Table 1).

Figure 10*B-a* and *b* shows 2-D surface plots of the 2-D probability distribution function (Eq. 5) fitted to the experimental 2-D dwell-time histograms for 0 and 10 mM Mg^{2+} shown in Fig 10*A-a* and *b*, respectively. The 2-D probability distribution functions are well fitted to the experimental 2-D dwell-time histograms for 0 and 10 mM Mg^{2+} with two open and three closed exponential components.

Table 1. Values of parameters in the 2-D probability distribution function, pdf_{2D}.

$[Ca^{2+}]_i$ $[Mg^{2+}]_i$	$10^{-5.5}$ M 0 mM	$10^{-5.5}$ M 10 mM	10^{-2}M 0 mM
τ_{O1}	1.97 ± 0.19	6.61 ± 2.97	8.83 ± 2.12*
τ_{O2}	5.12 ± 0.85	13.06 ± 3.44	17.64 ± 3.80*
τ_{C1}	0.59 ± 0.04	0.54 ± 0.03	0.44 ± 0.03*
τ_{C2}	7.23 ± 1.63	10.00 ± 5.62	1.99 ± 0.11*
τ_{C3}	34.29 ± 12.38	106.32 ± 23.04*	12.66 ± 1.91
$Vij_{1\text{-}1}$	0.05 ± 0.02	0.27 ± 0.06*	0.19 ± 0.04*
$Vij_{1\text{-}2}$	0.10 ± 0.03	0.04 ± 0.03	0.05 ± 0.04
$Vij_{1\text{-}3}$	0.20 ± 0.03	0.08 ± 0.02*	0.01 ± 0.01*
$Vij_{2\text{-}1}$	0.34 ± 0.04	0.55 ± 0.04*	0.63 ± 0.05*
$Vij_{2\text{-}2}$	0.17 ± 0.02	0.04 ± 0.02*	0.13 ± 0.04
$Vij_{2\text{-}3}$	0.16 ± 0.05	0.05 ± 0.03	0.02 ± 0.01*

Significantly different ($P < 0.05$) from values obtained in the absence of Mg^{2+} at $10^{-5.5}$ M Ca^{2+}.

Table 2. Values of rate constants in gating model I.

$[Ca^{2+}]_i$ $[Mg^{2+}]_i$	$10^{-5.5}$ M 0 mM	$10^{-5.5}$ M 10 mM	10^{-2} M 0 mM
$k_{C32}(s^{-1})$	113.9 ± 24.33	28.50 ± 5.58*	2632 ± 405.7*
k_{C23}	355.1 ± 90.03	320.3 ± 55.01	411.7 ± 75.85
k_{C21}	1.43 ± 0.35	0.79 ± 0.18	40.11 ± 3.40*
k_{C12}	17.00 ± 4.20	15.81 ± 1.58	17.33 ± 1.37
β_1	319.5 ± 44.06	283.7 ± 55.98	341.7 ± 38.69
α_1	297.3 ± 25.89	200.6 ± 55.94	87.07 ± 12.88*
β_2	3248 ± 292.4	2242 ± 127.3*	2164 ± 228.2*
α_2	141.0 ± 33.77	138.8 ± 34.74	88.58 ± 17.96
k_{O12}	0.78 ± 0.26	26.20 ± 6.59*	20.35 ± 2.846*
k_{O21}	3.79 ± 1.53	3.13 ± 0.77	2.76 ± 0.57

*Significantly different ($P < 0.05$) from values obtained in the absence of Mg^{2+} at $10^{-5.5}$ M Ca^{2+}.

Figure 11*A-a* and *b* shows the 2-D dwell-time histograms reproduced from fitted values of parameters in gating model I (Table 2). Gating model I well reproduced the experimental 2-D dwell-time distributions for 0 and 10 mM Mg^{2+}. Note the good agreement between the experimental data and the simulated data in the 1-D open and closed dwell-time distributions (Fig. 11*B*).

Table 2 summarizes the effect of 10 mM Mg^{2+} at a $[Ca^{2+}]_i$ of $10^{-5.5}$ M on the rate constants in gating model I. The application of 10 mM Mg^{2+} had two major effects, that is, it increased the rate constant from O_1 to 62, k_{O12}, by ~35-fold and decreased the rate constant from C_3 to C_2, k_{C32}, by ~0.25-fold. The rate constant from C_1 to O_2, β_2, was also decreased significantly; however, the extent of the change (~0.66-fold) was much smaller than that for k_{O12} and k_{C32} (*see* Discussion). The Mg^{2+}-induced increase in k_{O12} suggests that Mg^{2+} binds to the channel in the O_1 state and accelerates the transition from O_1 to O_2. This is consistent with our experimental results for the K_{Mg}–P_{min} relationship (Fig. 7), which suggests that the binding of Mg^{2+} to BK channel occurs in its open conformation. The Mg^{2+}-induced decrease in k_{C32} suggests that the point at which the binding of Ca^{2+} to the BK channel is competitively inhibited by Mg^{2+} might be the transition from C_3 to C_2 (*see* Discussion). These dual effects of Mg^{2+} on the gating of BK channels are consistent with the recent finding that Mg^{2+}-binding sites are low-affinity non-selective sites for divalent cations distinct from the conventional high-affinity Ca^{+}-binding sites (Shi & Cui, 2001; Zhang et al. 2001; Xia, Zeng & Lingle, 2002). The O_1-O_2 transition would be mediated by the low-affinity non-selective site and the C_3-C_2 transition would be mediated by the high-affinity Ca^{2+}-binding site (*see* Discussion).

Discussion

The present study has demonstrated that an increase in $[Mg^{2+}]_i$ suppressed current amplitude, and enhanced P_o with an extension of the mean open time in the BK channel of RPTECs. Regarding the internal Mg^{2+}-induced suppression, several investigators

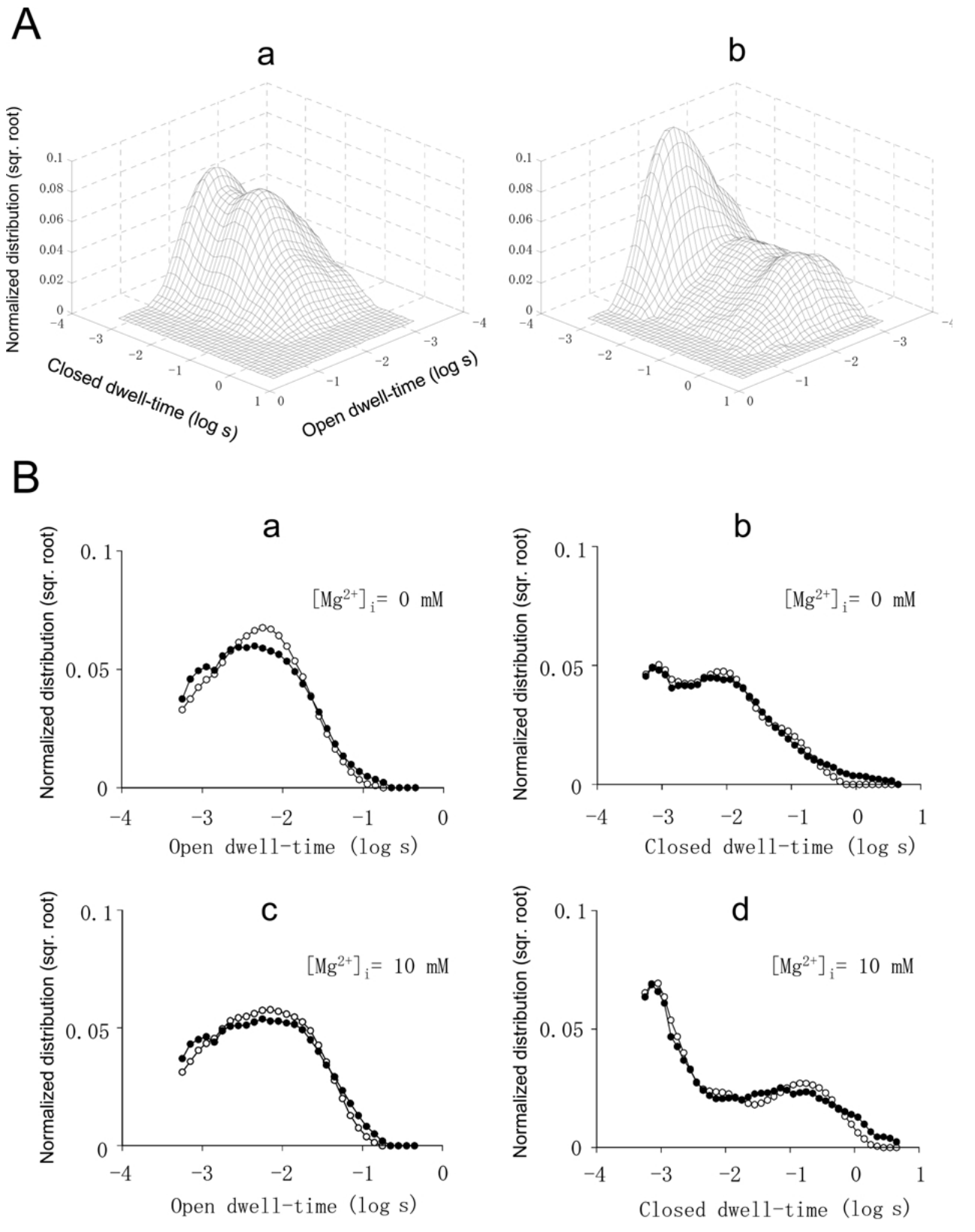

Fig. 11. Two-dimensional analysis of the effects of Mg^{2+} on RPTEC BK channel gating (II). (*A*) 2-D dwell-time distribution of adjacent open and closed intervals simulated for the experimental data shown in Fig. 10*A*, using kinetic scheme I with (*a*) 0 mM and (*b*) 10 mM Mg^{2+}. Parameters are summarized in Table 2. (*B*) Comparisons of 1-D (*a*, *c*) open and (*b*, *d*) closed dwell-time distributions between (●) experimental and (○) simulated data with (*a*, *b*) 0 and (*c*, *d*) 10 mM Mg^{2+}.

have already reported that the suppression becomes greater as the $[Mg^{2+}]_i$ increases and as the V_m is made more positive (Tabcharani & Misler, 1989; Ferguson, 1991; Zhang et al., 1995; Morales et al., 1996; Wachter & Turnheim, 1996; Bringmann et al., 1997; Kazachenko & Chemeris, 1998). We obtained similar results regarding the Mg^{2+}-induced suppression of currents (Fig. 1). Although this suppression is significant, in the present study we focused on another effect of Mg^{2+} on the BK channel. Mg^{2+} enhances the channel's activity while increasing the Hill coefficient for the Ca^{2+}-dependent activation of channels.

Voltage-Insensitive Action of Mg^{2+} on P_o in the BK Channel

It has been demonstrated that internal Mg^{2+} has a stimulatory effect on the activity of the BK channels in several animal tissues (Golowasch et al., 1986; Squire & Petersen, 1987; Oberhauser et al., 1988; McLarnon & Sawyer, 1993; Zhang et al., 1995; Morales et al., 1996; Bringmann et al., 1997; Kazachenko & Chemeris, 1998) including a cloned BK channel, mslo1 (Shi & Cui, 2001; Zhang et al., 2001; Shi et al., 2002; Xia et al., 2002). The BK channel in cultured human kidney cells, RPTECs, was also activated by internal Mg^{2+} as demonstrated in Fig. 1*A*. Thus, internal Mg^{2+} would be one of the factors regulating the BK channel family. As for the nature of the Mg^{2+}-induced increase in P_o, we showed that the effect of Mg^{2+} on the P_o of the BK channel in RPTECs at various $[Ca^{2+}]_i$ was not dependent on V_m, since the Boltzmann constant (α) of the P_o–V_m relationship was not significantly altered (Figs. 2 and 3*B*). Similar data were reported for BK channels of rat skeletal muscle (Oberhauser et al., 1988), rat smooth muscle (Zhang et al., 1995), and mslol (Shi & Cui, 2001; Zhang et al., 2001). Thus it is suggested that the Mg^{2+}-mediated enhancement of BK channel activity is independent of voltage. Furthermore, we found in this study that the Mg^{2+}-induced shift in the P_o–V_m relationship or changes in response to a rise in the $[Mg^{2+}]_i$ was diminished when the $[Ca^{2+}]_i$ was lowered to $10^{-5.5}$ or 10^{-6} M (Figs. 2 and 3*A*). Thus, it is conceivable that the effect of Mg^{2+} on P_o would be altered by the $[Ca^{2+}]_i$.

Involvement of Sensitivity to Ca^{2+} in Mg^{2+}-Mediated Activation of Channels

Several investigators have examined the effect of raising the $[Mg^{2+}]_i$ on the Ca^{2+}-dependent activation of BK channels to clarify the interaction between Mg^{2+} and Ca^{2+} (Golowasch et al., 1986; Oberhauser et al., 1988; Zhang et al., 1995; Morales et al., 1996; Kazachenko & Chemeris, 1998; Shi & Cui, 2001; Zhang et al., 2001; Shi et al., 2002). It was found that raising the $[Mg^{2+}]_i$ shifted the Ca^{2+}-activation curve in the direction of a lower $[Ca^{2+}]_i$, and elevated the Hill coefficient for binding of Ca^{2+}. Because the Hill coefficient for Ca^{2+} rose as the $[Mg^{2+}]_i$ increased, it has been suggested that Mg^{2+} enhanced the sensitivity of the BK channels to Ca^{2+} (Golowasch et al., 1986; Oberhauser et al., 1988; Kazachenko & Chemeris, 1998). Furthermore, Golowasch et al., (1986) and Oberhauser et al., (1988) proposed that raising the $[Mg^{2+}]_i$ revealed Ca^{2+}-binding sites that were masked in the absence of Mg^{2+}. Our data also suggested the possibility that the Mg^{2+}-mediated enhancement of P_o was induced by an increase in the sensitivity of the channel to Ca^{2+}, since raising the $[Mg^{2+}]_i$ increased the Hill coefficient for Ca^{2+}, and enhanced the sigmoidicity of the P_o–$[Ca^{2+}]_i$ relationship (Fig. 4*A*). However, Shi and Cui (2001) and Zhang et al., (2001) demonstrated that the Mg^{2+}-induced enhancement of the BK channel's activity was independent of sensitivity to Ca^{2+}, since Mg^{2+} was able to activate the channel even in the absence of Ca^{2+}. Furthermore, experiments using a mutation of the mslo1 channel revealed that Mg^{2+}-sensitive sites located in the RCK domain were distinct from high-affinity Ca^{2+}-binding sites (Shi et al., 2002).

To clarify whether the effect of Mg^{2+} on P_o was mediated by changes in the sensitivity of the BK channel to Ca^{2+}, we attempted to compare the changes in gating kinetics of single-channel currents in response to increase in the $[Mg^{2+}]_i$ and $[Ca^{2+}]_i$. We found that raising the $[Mg^{2+}]_i$ from 0 to 10 mM at 10^{-5} M $[Ca^{2+}]_i$ increased the P_o mainly by lengthening the mean open time, whereas raising the $[Ca^{2+}]_i$ from 10^{-5} to 10^{-4} M in the absence of Mg^{2+} increased P_o mainly by shorting the mean closed time, even though both these manipulations resulted in a similar increase in P_o (Fig. 5). The results indicate that the increase in P_o induced by raising the $[Mg^{2+}]_i$ was distinct from that induced by raising the $[Ca^{2+}]_i$. Therefore, it is suggested that the Mg^{2+}-induced enhancement of BK channel activity in RPTECs was independent of sensitivity to Ca^{2+}, at least under these conditions. These findings are supported by the view that the Mg^{2+}-sensitive sites were different from the high-affinity Ca^{2+}-binding sites (Shi et al., 2002), although why the Hill coefficient for Ca^{2+} was altered by changes in the $[Mg^{2+}]_i$ remains to be answered. We will discuss this question below.

Possible Mechanism for Mg^{2+}-induced Extension of the Open Time

As mentioned above, the Mg^{2+}-induced increases in P_o would be independent of the Ca^{2+}-induced activation of the channels. It has been revealed using a cloned BK channel that the Ca^{2+}-induced activation was mediated by high-affinity Ca^{2+}-binding sites located in the large cytosolic carboxy terminus of the

Table 3. Values of parameters for reproducing Mg^{2+}-induced enhancement in the two-tiered, 10-state gating scheme C-1

α_c^0	1×10^9 $M^{-1}s^{-1}$
$K_{Ca(C)}$	15 μM
$K_{Mg(C)}$	10 mM
β_c	1.5×10^4 s^{-1}
α_o^0	1×10^9 $M^{-1}s^{-1}$
β_o	1.5×10^5 s^{-1}
($K_{Ca(O)}$	150 μM)
($K_{Mg(O)}$	150 μM)
δ_0	7.4×10^{-3} s^{-1}
δ_1	1.3×10^{-1} s^{-1}
δ_2	20 s^{-1}
δ_3	200 s^{-1}
δ_4	800 s^{-1}
γ_0	3.7×10^3 s^{-1}
γ_1	3.7×10^3 s^{-1}
γ_2	1000 s^{-1}
γ_3	500 s^{-1}
γ_4	50 s^{-1}

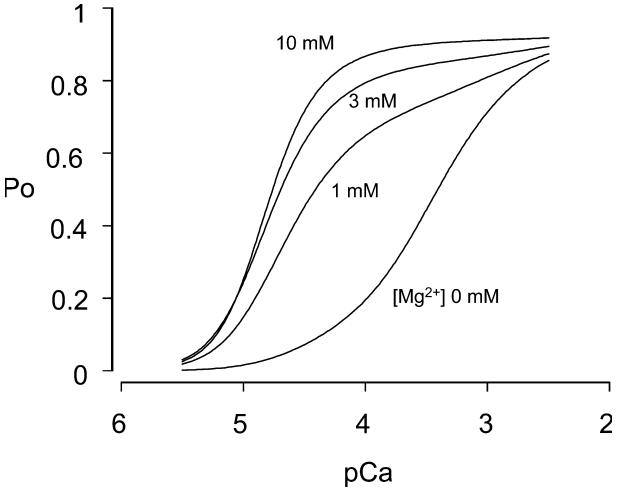

Fig. 12. Mg^{2+}-induced enhancement of Ca^{2+}-dependent channel activity (P_o) at $V_m = -45$ mV reproduced from the two-tiered, 10-state MWC gating scheme C-1 shown in Appendix 3. Mg^{2+} concentrations are shown in the figure. Values of parameters used for calculations are shown in Table 3.

channel (Wei et al., 1994; Schreiber & Salkoff, 1997; Schreiber et al., 1999; Bian et al., 2001). More recently, experiments using a mutated mslo1 channel demonstrated that Mg^{2+}-sensitive sites are located in the RCK domain, which were distinct from the high-affinity Ca^{2+}-binding sites (Shi et al., 2002).

In this study, we demonstrated that raising the $[Mg^{2+}]$ increased the P_o with a marked extension of the open time of the channel, different from Ca^{2+}-induced activation (Fig. 5); the extent of the Mg^{2+}-induced increase in P_o was dependent on the P_o under Mg^{2+}-free conditions ($P_{o(0Mg)}$) not on the $[Ca^{2+}]_i$ or voltage (Fig. 6); and the binding of Mg^{2+} to the BK channel occurred only when the channel was open (Fig.6). Moreover, the 2-D dwell-time analysis (Figs. 10 and 11) showed that Mg^{2+} accelerated the transition from O_1 to O_2 in gating model I (Table 2). Thus it is suggested that Mg^{2+} acts on the BK channel to bind to and stabilize its open conformation, which results in an extension of the mean open time (*see* scheme II). In other words, an open conformation produced by either $[Ca^{2+}]_i$ or voltage was required to elicit the action of Mg^{2+} on the open time of the BK channel.

Suppression of Mg^{2+}-mediated Activation of Channels at a Relatively Low $[Ca^{2+}]_i$

The present study demonstrated that the Mg^{2+}-mediated shift in the P_o–V_m relationship or change in $V_{1/2}$ was diminished at a $[Ca^{2+}]_i$ of $10^{-5.5}$ and 10^{-6} M (Figs. 2*D* and 3*A*). This means that the Mg^{2+}-induced enhancement of P_o is suppressed at a relatively low $[Ca^{2+}]_i$ (10^{-6}–$10^{-5.5}$ M). Regarding this mechanism, at least two possibilities are conceivable.

One is that the Mg^{2+}-induced opening of the channel requires a relatively high $[Ca^{2+}]_i$, and the Mg^{2+}-induced enhancement is diminished at a relatively low $[Ca^{2+}]_i$. Indeed, our finding that the degree of the Mg^{2+}-induced elevation of P_o depends on $P_{0(0Mg)}$ (Fig. 6) was obtained when the $[Ca^{2+}]_i$ was relatively high (10^{-5}–10^{-3} M). However, as mentioned above, raising the $[Mg^{2+}]_i$ prolonged the open time of the channel even at a relatively low $[Ca^{2+}]_i$ (Fig. 7). Since the major effect of Mg^{2+} on channel activity is considered to be a lengthening of the open time, the diminished effect of Mg^{2+} on the enhancement of P_o was not due to the diminished actions of Mg^{2+}.

The other possibility is that raising the $[Mg^{2+}]_i$ competitively inhibited the binding of Ca^{2+} to the high affinity-sites, which also resulted in a suppression of the increase in P_o. This possibility is supported by evidence that raising the $[Mg^{2+}]_i$ extended the mean open time with a simultaneous extension of the closed time at a relatively low $[Ca^{2+}]_i$ (Fig. 7), which resulted in a suppression of the increase in P_o. Since raising the $[Ca^{2+}]_i$ induced a shortening of the closed time, or lowering the $[Ca^{2+}]_i$ extended the closed time as shown in Fig. 5*B*, extension of the closed time at a high $[Mg^{2+}]_i$ might be induced by competitive inhibition of the binding of Ca^{2+} to the high-affinity sites. Two papers showed that a high concentration of Mg^{2+} competitively inhibits high-affinity Ca^{2+}-binding sites (Shi & Cui, 2001; Zhang et al., 2001). In this study, the 2-D dwell-time analysis (Figs. 10 and 11) showed that Mg^{2+} inhibited the transition from C_3 to C_2 in gating model I, which was thought to be a Ca^{2+}-dependent step (Rothberg & Magleby, 1999, 2000) (Table 2). Thus it is likely that at a relatively low

$[Ca^{2+}]_i$, raising the $[Mg^{2+}]_i$ extends the closed time through competitive inhibition of the binding of Ca^{2+} to the high-affinity sites, which results in a diminished action of Mg^{2+} on P_o.

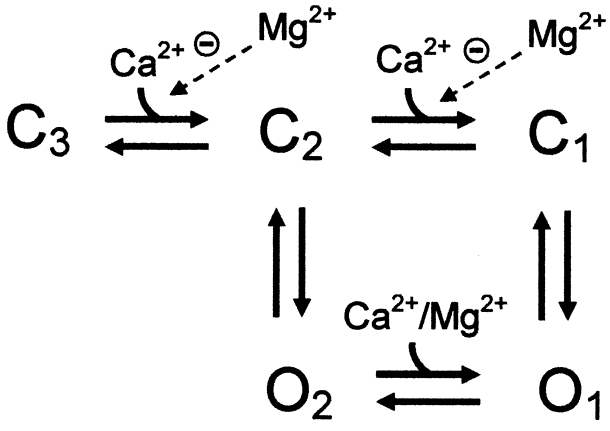

(Scheme II)

Possible Mechanism Underlying Mg^{2+}-induced Changes in Ca^{2+}-dependent BK Channel Activation

The Mg^{2+}-induced change in the Hill coefficient for the P_o–$[Ca^{2+}]_i$ relationship (Fig. 4A) appeared to be induced by a combination of the competitive inhibition of the binding of Ca^{2+} to the high-affinity Ca^{2+} sites by Mg^{2+} in closed channels and the mutual binding of Mg^{2+} to the low-affinity Mg^{2+}/Ca^{2+} sites in open channels. We investigated whether the dual effects of Mg^{2+} can reproduce the Mg^{2+}-induced change in the Hill coefficient during the Ca^{2+}-dependent activation. We first developed a two-tiered, 10-state, Monod-Wyman-Changeux (MWC) scheme C-1 with incorporating the assumption of a competitive inhibition of the binding of Ca^{2+} to the high-affinity site by Mg^{2+} and the binding of Mg^{2+} to the low-affinity Mg^{2+}/Ca^{2+} site (*see* Appendix 3 for detail).

Figure 12 shows the P_o–$[Ca^{2+}]_i$ relationships calculated from gating scheme C-1 (Appendix 3) with the set of parameters shown in Table 3. The C-1 model could quantitatively approximate the experimental P_o–$[Ca^{2+}]_i$ relationships shown in Fig. 4*A*.

These results support the idea that the Mg^{2+}-induced changes in BK channel activity with the increase in the Hill coefficient during Ca^{2+}-dependent activation is caused by combination of the competitive inhibition of Ca^{2+} binding by Mg^{2+} in a closed state and the activation by Mg^{2+} binding to the Mg^{2+}/Ca^{2+} site in an open state. We also found that the competitive inhibition affected the increase in the Hill coefficient significantly at a $[Ca^{2+}]_i$ lower than 10^{-5} M (Fig. 12).

Possible Molecular Mechanism of Mg^{2+}-Enhancement

It is suggested that BK channels are regulated by at least three distinct divalent cation-dependent regulatory mechanisms in the COOH terminus of the α subunit (Xia et al., 2002; Zeng et al., 2005). The so-called "Ca^{2+} bowl" and the D362/D367-related high-affinity Ca^{2+}-binding site, which account for the physiological regulation by micromolar Ca^{2+}, and the E374/E399-related low-affinity Ca^{2+}/Mg^{2+}-binding site, which may mediate the physiological regulation by millimolar Mg^{2+}, were defined in the first RCK domain of the mSlo 1 α subunit (Shi et al., 2002; Xia et al., 2002; Zheng et al., 2005). The RCK domains are believed to form a gating ring and produce the conformational changes required for opening of the channel (Jiang et al., 2001, 2002, Krishnamoorthy et al., 2005). The present study suggests that Mg^{2+} binds to the Ca^{2+}/Mg^{2+} site in an open channel and the binding is dependent on the closed-open conformation, not the concentration of Ca^{2+} or membrane potential (Fig. 7). Therefore the low-affinity Ca^{2+}/Mg^{2+}-binding site might be accessible only when the channel is in the open conformation. If this is the case, the mechanism of the enhancement by Mg^{2+} may be as follows: 1) the binding of Ca^{2+} to the high-affinity Ca^{2+} sites and/or depolarization induce a conformational change in the RCK gating ring; 2) this conformational change causes the BK channel to adopt a more activated state; 3) once the channel opens, a conformational change makes the low-affinity Ca^{2+}/Mg^{2+}-binding site in the RCK domain accessible; and 4) the binding of Mg^{2+} to the Ca^{2+}/Mg^{2+}-site makes the open conformation more stable. On the other hand, the "Ca^{2+} bowl" and the D362/D367-related high-affinity site might be accessible when the RCK gating ring is in the closed state.

Contribution of β Subunits to Mg^{2+}-induced Activation

BK channels are a protein complex formed by two integral membrane subunits, the pore-forming α-subunit and a regulatory β subunit. BK channels have diverse physiological properties with a tissue-specific distribution and four isoforms (β 1–4) of the β subunit, which provide BK channel diversity (*see* Orio et al., 2002 for review). The β1 and β2 subunits significantly increase the apparent Ca^{2+}-dependence of activation (McManus et al., 1995; Wallner et al., 1999; Xia, Ding & Lingle 1999); ß2 (Wallner, Meera & Toro, 1999; Xia et al., 1999) and β 3a–c (Xia et al., 2000; Uebele et al., 2000) subunits induce inactivation of BK channels; β3d subunits affect neither the apparent sensitivity to Ca^{2+} nor the gating kinetics (Meera, Wallner & Toro, 2000); and β4 subunits

decrease the apparent sensitivity to Ca^{2+} (Brenner et al., 2000b; Meera et al., 2000) and may regulate the function of BK channels phosphorylation-dependently (Jin et al., 2002). More recently Qian & Magleby (2003) reported that the presence of β1 subunit influenced the Mg^{2+}-dependent effect on channel activity, i.e., Mg^{2+} inhibits the activity of BK channels in the presence of the β1 subunit at physiologically relevant levels of Ca^{2+}

In our preliminary RT-PCR experiments, RPTECs expressed the mRNAs of the β2, β3c and β4 subunits (*data not shown*). Although it is still unknown which, if any, subtype of the β subunit contributes to the formation of RPTEC BK channels expressed in the plasma membrane, the actions of Mg^{2+} on RPTEC BK channels were very similar to those on mSlo channels formed by the α-subunit only (Shi & Cui, 2001; Zhang et al 2001; Xia et al. 2002).

Conclusion

In the present study, we demonstrated that in the BK channel endogenously expressed in RPTECs, internal Mg^{2+} elevated P_o mainly by extending open time, and simultaneously lengthened closed time at a relatively low $[Ca^{2+}]_i$. We investigated the mechanism for the Mg^{2+}-mediated changes in the open and closed times of the BK channel. It is suggested that the Mg^{2+}-induced changes involve a combination of the competitive inhibition of the binding of Ca^{2+} to the high-affinity Ca^{2+} sites by Mg^{2+} in closed channels and the mutual binding of Mg^{2+} to the low-affinity Mg^{2+}/Ca^{2+} sites in open channels, the former inducing an extension of the closed time, and the latter inducing an extension of the open time. Thus, the internal Mg^{2+} increased the Hill coefficient for the Ca^{2+}-dependent activation of the channel without changing the gating charge, which is consistent with recent studies using cloned BK channels (Shi & Cui, 2001; Zhang et al., 2001; Shi et al., 2002; Xia et al., 2002). However, the role of the BK channels in RPTECs is still unknown, since the current of this channel is weak in intact cells even though $[Mg^{2+}]_i$ would have a stimulatory effect on the channel's activity. Further study will be necessary to clarify the physiological significance of BK channels in the functions of the kidney.

We gratefully acknowledge Prof. K. L. Magleby (University of Miami) for providing the program for analyzing 2-D dwell-time. This study was partly supported by a grant from the Japan Society for the Promotion of Science to Y.S. (15590196).

Appendix 1

Simplification of the Gating Model

Rothberg & Magleby (1999, 2000) proposed a general 50-state two-tiered gating model of BK channels consisting of 25 closed states on the upper tier and 25 open states on the lower tier, which could approximate both dwell-time distributions from low to high $Ca^{2+}{}_i$. To analyze the effects of Mg^{2+} on the gating of RPTEC BK channels, we employed this model but reduced the number of states.

We recorded the single-channel current for 2-D dwell-time distribution analysis at a fixed voltage of 15 mV (Fig. 8). At a fixed voltage, the original two-tiered kinetic model involved five states in the open and closed tiers, respectively (Rothberg & Magleby, 1999, 2000) (see the gray + black part in scheme A-1). Under all the conditions of $[Ca^{2+}]_i$ and $[Mg^{2+}]_i$ adopted in this study, the 1-D open- and closed-time distributions could be fitted by two and three exponential components, respectively (*see* Figs. 6*A* and 9). Therefore we reduced the states in the model to two open and three closed states because of minimal numbers of underlying 2-D exponential components. This means that we omitted the states with a very low occupancy probability and/or very short mean lifetime under the experimental conditions used for the kinetic analysis. Because we used relatively high concentrations of $Ca^{2+}{}_i$ at which P_o was ~0.3, the reduced two-tiered two-open and three-closed state model might correspond to the right end (higher Ca^{2+} concentration end) of the Rothberg & Magleby model (*see* the black part in scheme A-1).

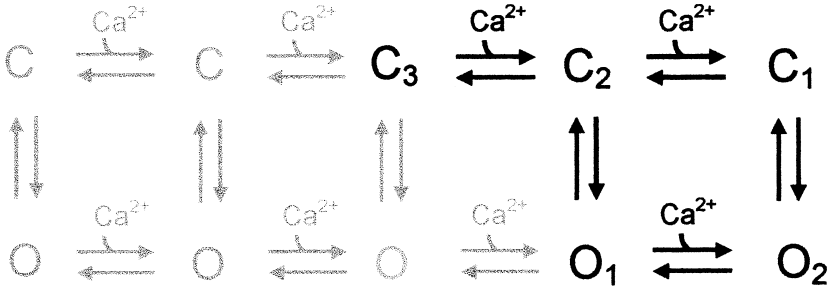

(Scheme A-1)

An Iterative Estimation of Rate Constants

To estimate the rate constants in gating model I from the 2-D dwell-time distribution, we employed an iterative simulation method similar to that described by Magleby & Weiss (1990).

First, an idealized single-channel current including 300,000 opening-closing event pairs was generated according to the proposed gating scheme I, with no noise and an unlimited time resolution. The idealized single-channel current was sampled at 10 kHz by superimposing Gaussian noise (Press et al., 1992) and low-pass filtered at 2 kHz with a digital Gaussian filter (Colquhoun & Sigworth, 1995). The amplitude of the Gaussian noise was adjusted to show a root-mean-square amplitude in the final output similar to that observed in closed states in our experimental current recordings (~0.8 $pA_{p\text{-}p}$ at 2 kHz filtered). The durations of open and closed intervals in the simulated single-channel currents were measured with a half-amplitude threshold analysis and binned into the 2-D dwell-time histograms in a manner identical to that used to analyze the experimental data.

The most likely rate constants were determined from direct likelihood comparisons of the simulated 2-D dwell-time distribution with the 2-D dwell-time distribution best-fitted to the experimental 2-D dwell-time distribution. The fitting of data was restricted to intervals with a duration greater than two-fold the dead times. To simplify the writing, the text will refer to the fitting of the (smoothed) 2-D dwell-time distributions (surface plots) presented in the figures (*see* Method), when, in reality, the non-smoothed 2-D frequency histograms were fitted.

Note that the simplification we performed on the general 50-state two-tiered scheme of BK channel gating and original 2-D dwell-time analysis described by Rothberg & Magleby (1999, 2000) should somehow reduce the accuracy of estimates of model parameters.

Appendix 2

An Open Channel Mg^{2+}-Binding Scheme for Mg^{2+}-dependent Activation

To qualify the interaction of Mg^{2+} with the BK channel from the P_o data with and without Mg^{2+}, we employed a simple gating scheme in which Mg^{2+} could bind to the channel in its open conformation and stabilize it, as follows:

$$\underset{\vdots}{\overset{\text{(closed)}}{C}} \underset{\alpha}{\overset{\beta}{\longleftrightarrow}} \underset{\vdots}{\overset{\text{(open)}}{O}} + Mg^{2+} \underset{k_{off}}{\overset{k_{on}}{\longleftrightarrow}} \underset{\vdots}{\overset{\text{(Mg-open)}}{O \cdot Mg^{2+}}} \qquad (Scheme B-1)$$

According to the open-channel stabilization scheme B-1, the open probability in the presence of Mg^{2+} (P_oMg) is derived as follow:

$$P_{oMg} = P_{o(0Mg)} + \frac{1 - P_o(0Mg)}{1 + \left(\frac{K_{Mg}}{[Mg^{2+}]}\right)} \qquad (B1)$$

where $P_{o(0Mg)}$ is the open probability in the absence of Mg^{2+} and K_{Mg} is the apparent dissociation constant of Mg^{2+} binding to the channel, described as follows:

$$K_{Mg} = \left(\frac{1}{P_{o(0Mg)}}\right) \cdot \left(\frac{K_{off}}{K_{on}}\right) = \frac{K^0_{Mg}}{P_{o(0Mg)}} \qquad (B2)$$

where K^0_{Mg} is the value of K_{Mg} under the conditions where the open probability is equal to 1 in the absence of Mg^{2+}.

From Eq. B2

$$\log K_{Mg} = \log K^0_{Mg} - \log P_{o(0Mg)} = \log K^0_{Mg} - \log P_{min} \qquad (B3)$$

where P_{min} is the open probability in the absence of Mg^{2+} used in Eq. 4

Therefore K_{Mg} is in inverse proportion to $P_{o(0Mg)}$ in the open-channel stabilization scheme B-1. This means that the log-log plots of K_{mg} against P_{min} should show a slope of −1, which is consistent with our experimental data (Fig. 7 *A, B*).

In the case where state-independent binding of Mg^{2+} opened the closed channel and stabilized the open channel, K_{Mg} should be independent of $P_{o(0Mg)}$ (equation not shown). Assuming that Mg^{2+} could bind to the channel in its closed conformation and open the channel, K_{Mg} should be described as follows (derivation not shown):

$$\log K_{Mg} = \log K^0_{Mg} - \log P_{o(0Mg)} = \log K^0_{Mg} - \log (1 - P_{min}) \qquad (B4)$$

In this case, the log-log plots of K_{Mg} against P_{min} should show a positive slope, which is inconsistent with our experimental data (Fig. 7*A, B*).

Appendix 3

A Two-Tiered, 10-State Gating Scheme for Reproducing Mg^{2+}-induced Enhancement

To reproduce the Mg^{2+}-induced enhancement of P_o, we developed a two-tiered, 10-state Monod-Wyman-Changeux gating scheme (Cox et al., 1997) with the assumption of a competitive inhibition of the binding of Ca^{2+} to the high-affinity Ca^{2+} sites by Mg^{2+} in closed channels (Eq. C8) and a mutual binding of Mg^{2+} to the low-affinity Mg^{2+}/Ca^{2+} sites in open channels (Eq. C9).

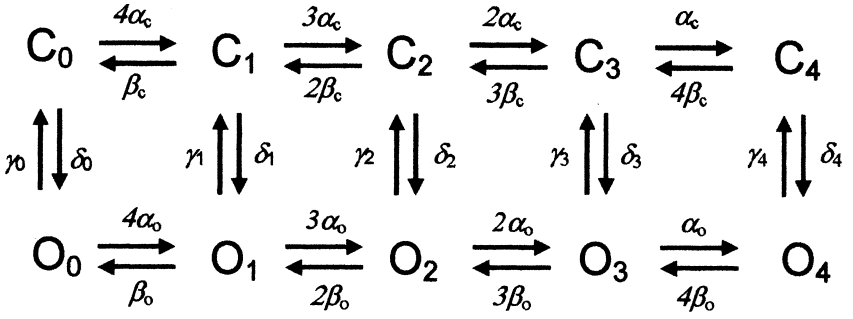

(Scheme C-1)

where C_i and O_i, are closed and open channels with a number *i* (0–4) of Ca^{2+} (or Mg^{2+}) ions binding to the BK channel; α_c and β_c, and α_0 and β_0 are the apparent binding and unbinding rates of Ca^{2+} to BK channels in closed and open states; γ_i and δ_i are transition rates from O_i, to C_i and from C_i, to O_i.

Derivation of the Apparent On-Rate of Ca^{2+} Binding under Competitive Inhibition by Mg^{2+}

Assuming competitive inhibition between Ca^{2+} and Mg^{2+} as below:

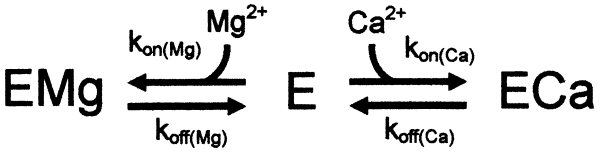

(Scheme C-2)

$$[EMg] + [E] + [ECa] = [E_0], \quad \text{(C1)}$$

$$k_{off(Ca)} \cdot [ECa] = k_{on(Ca)} \cdot [Ca^{2+}] \cdot [E], \quad \text{(C2)}$$

$$k_{off(Mg)} \cdot [ECa] = k_{on(Mg)} \cdot [Mg^{2+}] \cdot [E], \quad \text{(C3)}$$

From Eqs. |C1|–|C3|,

$$[E] = \frac{[E_0]}{1 + \frac{[Ca^{2+}]}{K_{Ca}} + \frac{[Mg^{2+}]}{K_{Mg}}} \quad \text{(C4)}$$

Where

$$K_{Mg} = k_{off(Mg)}/k_{on(Mg)}; K_{Ca} = k_{off(ca)}/k_{on(Ca)}$$

The apparent on-rate of Ca^{2+} binding in the presence of Mg^{2+}, α, is described by:

$$\alpha = k_{on(Ca)} \cdot [Ca^{2+}] \cdot [E] = k_{on(Ca)} \cdot [Ca^{2+}] \cdot \left(\frac{[E_0]}{1 + \frac{[Ca^{2+}]}{K_{Ca}} + \frac{[Mg^{2+}]}{K_{Mg}}} \right) \quad \text{(C5)}$$

In the absence of Mg^{2+},

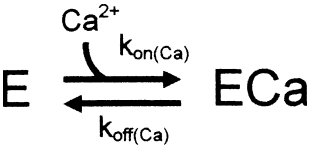

(Scheme C-3)

the on-rate of Ca^{2+} binding α^0, is described by:

$$\alpha^0 = k_{on(Ca)} \cdot [Ca^{2+}] \cdot [E] = k_{on(Ca)} \cdot [Ca^{2+}] \cdot \left(\frac{[E_0]}{1 + \frac{[Ca^{2+}]}{K_{Ca}}} \right), \quad \text{(C6)}$$

Therefore, from Eqs. C5 and C6,

$$\alpha = \alpha^0 \cdot [Ca^{2+}] \cdot \left(\frac{1 + \frac{[Ca^{2+}]}{K_{Ca}}}{1 + \frac{[Ca^{2+}]}{K_{Ca}} + \frac{[Mg^{2+}]}{K_{Mg}}} \right), \quad \text{(C7)}$$

Thus, the apparent Ca^{2+} -binding rate to the high-affinity Ca^{2+} sites in closed channels, α_c, is calculated as below:

$$\alpha_c = \alpha_c^0 \cdot [Ca^{2+}] \cdot \left(\frac{1 + \frac{[Ca^{2+}]}{K_{Ca(C)}}}{1 + \frac{[Ca^{2+}]}{K_{Ca(C)}} + \frac{[Mg^{2+}]}{K_{Mg(C)}}} \right), \quad \text{(C8)}$$

where α_c^0 is the apparent rate constant for the binding of Ca^{2+} to BK channels in a closed state without Mg^{2+}; and $K_{Ca(C)}$ ($= \beta_c/\alpha_c$) and $K_{Mg(c)}$ are dissociation constants for the binding of Ca^{2+} and Mg^{2+} to BK channels in the closed state.

The apparent Ca^{2+} binding rate to the low-affinity Mg^{2+}/Ca^{2+} sites in open channels, α_o, is calculated as below:

$$\alpha_o = \alpha_o^0 \cdot \left([Ca^{2+}] + [Mg^{2+}] \right), \quad \text{(C9)}$$

where α_o^0 is the rate constant for the binding of Ca^{2+} and Mg^{2+} to BK channels in an open state.

Calculation of P_o in Scheme C-1

P_o is calculated by using the Q-matrix method (Colquhoun & Hawkes, 1995). Values of the parameters (Table 3) were determined from our P_o–$[Ca^{2+}]_i$ data

(Fig. 4*A*) referring to the values reported by Cox et al. (1997).

References

Adelman, J.P., Shen, K.-Z., Kavanaugh, M.P., Warren, R.A., Wu, Y.-N, Lagrutta, A., Bond, C.T., North, A. 1992. Calcium-activated potassium channels expressed from cloned complementary DNAs. *Neuron* **9:**209–216

Atkinson, N.S., Robertson, G.A., Ganetzky, B. 1991. A component of calcium-activated potassium channels encoded by the *Drosophila slo* locus. *Science* **253:**551–555

Barrett, J.N., Magleby, K.L., Pallotta, B.S. 1982. Properties of single calcium-activated potassium channels in cultured rat muscle. *J. Physiol.* **331:**211–230

Bian, S., Favre, I, Moczydlowski, E. 2001. Ca^{2+}-binding activity of a COOH-terminal fragment of the *Drosophila* BK channel involved in Ca^{2+}-dependent activation. *Proc. Natl. Acad. Sci. USA* **98:**4776–4781

Brenner, R., Jegla, T.J., Wickenden, A., Liu, Y., Aldrich, R.W. 2000b. Cloning and functional characterization of novel large conductance calcium-activated potassium channel β subunits, hKCNMB3 and hKCNMB4. *J. Biol. Chem.* **275:**6453–6461

Brenner, R., Perez, G.J., Bonev, A.D., Eckman, D.M., Kosek, J.C., Wiler, S.W., Patterson, A.J., Nelson, M.T., Aldrich, R.W. 2000a. Vasoregulation by the beta1 subunit of the calcium-activated potassium channel. *Nature* **407:**870–876

Bringmann, A., Faude, F., Reichenbach, A. 1997. Mammalian retinal glial (Müller) cells express large-conductance Ca^{2+}-activated K^+ channels that are modulated by Mg^{2+} and pH and activated by protein kinase A. *Glia* **19:**311–323

Butler, A., Tsunoda, S., McCobb, D.P., Wei, A., Salkoff, L. 1993. *mSlo*, a complex mouse gene encoding "maxi" calcium-activated potassium channels. *Science* **261:**221–224

Colquhoun, D., Hawkes, A.G. 1995. A Q-matrix cookbook: How to write only one program to calculate the single-channel and macroscopic prediction for any kinetic mechanism. Sakmann, B., Neher, E., (eds) Single-Channel RecordingPlenum Press-New York pp 589–633.

Colquhoun D., Sigworth F.J. 1995. Fitting and statistical analysis of single-channel records. *In:* B. Sakmann, E. Neher (eds). Single-Channel Recording Plenum Press, New York. pp. 483–587

Cox, D.H., Cui, J., Aldrich, R.W. 1997. Allosteric gating of a large conductance Ca-activated K^+ channel. *J. Gen. Physiol.* **110:**257–281

Cui, J., Aldrich, R.W. 2000. Allosteric linkage between voltage and Ca^{2+}-dependnet activation of BK-type mslo 1 K^+ channel. *Biochemistry* **39:**15612–15619

Cui, J., Cox, D.H., Aldrich, R.W. 1997. Intrinsic voltage dependence and Ca^{2+} regulation of *mslo* large conductance Ca-activated K^+ channels. *J. Gen. Physiol.* **109:**647–673

Curran-Everett, D. 2000. Multiple comparisons: philosophies and illustrations. *Am. J. Physiol.* **279:**R1–R8

Ferguson, W.B. 1991. Competitive Mg^{2+} block of a large-conductance, Ca^{2+}-activated K^+ channel in rat skeletal muscle Ca^{2+}, Sr^{2+}, and M^{2+} also block. *J. Gen. Physiol.* **98:**163–181

Golowasch, J., Kirkwood, A., Miller, C. 1986. Allosteric effects of Mg^{2+} on the gating of Ca^{2+}-activated K^+ channels from mammalian skeletal muscle. *J. Exp. Biol.* **124:**5–13

Hirano, J., Nakamura, K., Itazawa, S., Sohma, Y., Kubota, T., Kubokawa, M. 2002. Modulation of the Ca^{2+}-activated large conductance K^+ channel by intracellular pH in human renal proximal tubule cells. *Jpn. J. Physiol.* **52:**267–276

Horrigan, F.T., Cui, J., Aldrich, R.W. 1999. Allosteric voltage gating of potassium channels I. mSlo ionic currents in the absence of Ca^{2+}. *J. Gen. Physiol.* **114:**277–304

Hu, L., Shi, J., Ma, Z., Krishnamoorthy, G., Sieling, F., Zhang, G., Horrigan, F.T., Cui, J. 2003. Participation of the S4 voltage sensor in the Mg^{2+}-dependent activation of large conductance (BK) K^+ channels. *Proc. Natl. Acad. Sci. USA* **100:**10488–10493

Jiang, Y., Lee, A., Chen, J., Cadene, M., Chait, B.T., MacKinnon, R. 2002. Crystal structure and mechanism of a calcium-gated potassium channel. *Nature* **417:**515–522

Jiang, Y., Pico, A., Cadene, M., Chait, B.T., MacKinnon, R. 2001. Structure of the RCK domain from the *E. coli* K^+ channel and demonstration of its presence in the human BK channel. *Neuron* **29:**593–601

Jin, P., Weiger, T.M., Wu, Y, Levitan, I.B. 2002. Phosphorylation-dependent functional coupling of hSlo calcium-dependent potassium channel and its hbeta 4 subunit. *J. Biol. Chem.* **277:**10014–10020

Kazachenko, V.N., Chemeris, N.K. 1998. Modulation of the activity of Ca^{2+}-activated K^+ channels by internal Mg^{2+} in cultured kidney cells. *Vero. Membr. Cell. Biol.* **12:**489–511

Krishnamoorthy, G., Shi, J., Sept, D., Cui, J. 2005. The NH_2 terminus of RCK1 domain regulates Ca^{2+}-dependent BK_{Ca} channel gating. *J. Gen. Physiol.* **126:**227–241

Latorre, R., Oberhauser, A., Labarca, P., Alvarez, O. 1989. Varieties of calcium-activated potassium channels. *Annu. Rev. Physiol.* **51:**385–399

Magleby, K.L., Weiss, D.S. 1990. Estimating kinetic parameters for single channels with simulation. A general method that resolves the missed event problem and accounts for noise. *Biophys. J.* **58:**1411–1426

Martell A.E., Smith R. 1977. Critical Stability Constants. In: Other Organic Ligands, Vol 3. Plenum Press, New York

Marty, A. 1981. Ca-dependent K channels with large unitary conductance in chromaffin cell membranes. *Nature* **291:**497–500

McLarnon, J.G., Sawyer, D. 1993. Effects of divalent cations in the activation of a calcium-dependent potassium channel in hippocampal neurons. *Pfluegers Arch.* **424:**1–8

McManus, O.B. 1991. Calcium-activated potassium channels: regulation by calcium. *J. Bioenerg. Biomembr.* **23:**537–560

McManus, O.B., Helms, L.M., Pallanck, L., Ganetzky, B., Swanson, R., Leonard, R.J. 1995. Functional role of the β-subunit of high conductance calcium-activated potassium channels. *Neuron* **14:**645–650

Meera, P., Wallner, M., Toro, L. 2000. A neuronal beta subunit (KCNMB4) makes the large conductance, voltage- and Ca^{2+}-activated K^+ channel resistant to charybdotoxin and iberiotoxin. *Proc. Natl. Acad. Sci. USA.* **97:**5562–5567

Monod, J., Wyman, J., Changeux, J.P. 1965. On the nature of allosteric transitions: a plausible model. *J. Mol. Biol.* **12:**88–118

Morales, E., Cole, W.C., Remillard, C.V., Leblance, N. 1996. Block of large conductance Ca^{2+}-activated K^+ channels in rabbit vascular myocytes by internal Mg^{2+} and Na^+. *J. Physiol.* **495:**701–716

Neyton, J. 1995. A Ba^{2+} chelator suppresses long shut events in fully activated high-conductnace Ca^{2+}-dependent K^+ channels. *Biophys. J.* **71:**220–226

Oberhauser, A., Alvarez, O., Latorre, R. 1988. Activation by divalent cations of a Ca^{2+}-activated K^+ channel from skeletal muscle membrane. *J. Gen. Physiol.* **92:**67–86

Oiki, S., Okada, Y. 1987. Ca-EGTA buffer in physiological solutions (in Japanese). *Seitai-no-Kagaku* **38:**79–83

Orio, P., Rojas, P., Ferreira, G., Latorre, R. 2002. New disguises for an old channel: MaxiK channel beta-subunits. *News Physiol. Sci.* **17:**156–161

Press, W.H., Flannery, B.P., Teukolsky, S.A., Vetterling, W.T. 1992. Random Numbers. In: Numerical Recipes in FOR-

TRAN. 2nd edition, pp. 266–319, Cambridge University Press, New York

Piskorowski, R., Aldrich, R.W. 2002. Calcium activation of BK_{Ca} potassium channels lacking the calcium bowl and RCK domain. *Nature* **420:**499–502

Pluger, S., Faulhaber, J., Furstenau, M., Lohn, M., Waldschutz, R., Gollasch, M., Haller, H., Luft, F.C., Ehmke, H., Pongs, O. 2000. Mice with disrupted BK channel beta1 subunit gene feature abnormal Ca^{2+} spark/STOC coupling and elevated blood pressure. *Circ. Res.* **87:**E53–E60

Qian, X., Magleby, K.L. 2003. Beta1 subunits facilitate gating of BK channels by acting through the Ca^{2+}, but not the Mg^{2+}, activating mechanisms. *Proc. Natl. Acad. Sci. USA* **100:**10061–10066

Robitaille, R., Garcia, M.L., Kaczorowski, G.J., Charlton, M.P. 1993. Functional colocalization of calcium and calcium-gated potassium channels in control of transmitter release. *Neuron* **11:**645–655

Rothberg, B.S., Bello, R.A., Song, L., Magleby, K.L. 1996. High Ca^{2+} concentrations induce a low activity mode and reveal Ca^{2+}-independent long shut intervals in BK channels from rat muscle. *J. Physiol.* **493:**673–689

Rothberg, B.S., Bello, R.A., Magleby, K.L. 1997. Two-dimensional components and hidden dependencies provide insight into ion channel gating mechanisms. *Biophys. J.* **72:**2524–2544

Rothberg, B.S., Magleby, K.L. 1998. Kinetic structure of large-conductance Ca^{2+}-activated K^+ channels suggests that the gating includes transitions through intermediate or secondary states. A mechanism for flickers. *J. Gen. Physiol.* **111:**751–780

Rothberg, B.S., Magleby, K.L. 1999. Gating kinetics of single large-conductance Ca^{2+}-activated K^+ channels in high Ca^{2+} suggest a two-tiered allosteric gating mechanism. *J. Gen. Physiol.* **114:**93–124

Rothberg, B.S., Magleby, K.L. 2000. Voltage and Ca^{2+} activation of single large-conductance Ca^{2+}-activated K^+ channels described by a two-tiered allosteric gating mechanism. *Gen. Physiol.* **116:**75–99

Schreiber, M., Salkoff, L. 1997. A novel calcium-sensing domain in the BK channel. *Biophys. J.* **73:**1355–1363

Schreiber, M., Yuan, A., Salkoff, L. 1999. Transplantable sites confer calcium sensitivity to BK channels. *Nat. Neurosci.* **2:**416–421

Shi, J., Cui, L. 2001. Intracelmlar Mg^{2+} enhances the function of BK-type Ca^{2+}-activated K^+ channels. *J. Gen. Physiol.* **118:**589–605

Shi, J., Krishnamoorthy, G., Yang, Y., Hu, L., Chaturvedi, N., Harilal, D., Qin, J., Cui, J. 2002. Mechanism of magnesium activation of calcium-activated potassium channels. **18:**876–880

Sigworth, F.J., Sine, S.M. 1987. Data transformations for improved display and fitting of single-channel dwell time histograms. *Biophys. J.* **52:**1047–1054

Sohma, Y., Harris, A., Wardle, C.J.C., Gray, M.A., Argent, B.E. 1994. Maxi K^+ channels on human vas deferens epithelial cells. *J. Membr. Biol.* **141:**69–82

Song, L., Magleby, K.L. 1994. Testing for microscopic reversibility in the gating of maxi K^+ channels using two-dimensional dwell-time distributions. *Biophys. J.* **67:**91–104

Squire, L.G., Petersen, O.H. 1987. Modulation of Ca^{2+}- and voltage-activated K^+ channels by internal Mg^{2+} in salivary acinar cells. *Biochim. Biophys. Acta.* **899:**171–175

Tabcharani, J.A., Misler, S. 1989. Ca^{2+}-activated K^+ channel in rat pancreatic islet B cells: permeation, gating and blockade by cations. *Biochim. Biophys. Acta.* **982:**62–72

Uebele, V.N., Lagrutta, A., Wade, T., Figueroa, D.J., Liu, Y, McKenna, E., Austin, C.P., Bennett, P.B., Swanson, R. 2000. Cloning and functional expression of two families of β-subunits of the large conductance calcium-activated K^+ channel. *J. Biol. Chem.* **275:**23211–23218

Wachter, C., Turnheim, K. 1996. Inhibition of high-conductance, calcium-activated potassium channels of rabbit colon epithelium by magnesium. *J. Membrane Biol.* **150:**275–282

Wallner, M., Meera, P., Toro, L. 1999. Molecular basis of fast inactivation in voltage and Ca^{2+}-activated K^+ channels: a transmembrane β-subunit homolog. *Proc. Natl. Acad. Sci. USA* **96:**4137–4142

Wei, A., Solaro, C., Lingle, C., Salkoff, L. 1994. Calcium sensitivity of BK-type K_{Ca} channels determined by a separable domain. *Neuron* **13:**671–681

Woodhull, A.M. 1973. Ionic blockage of sodium channels in nerve. *J. Gen. Physiol.* **61:**687–708

Xia, X-M., Ding, J.P., Lingle, C.J. 1999. Molecular basis for the inactivation of Ca^{2+}- and voltage-dependent BK channels in adrenal chromaffin cells and rat insulinoma tumor cells. *J. Neurosci.* **19:**5255–5264

Xia, X-M., Ding, J., Zeng, X-H., Duan, K-L., Lingle, C.J. 2000. Rectification and rapid activation at low Ca^{2+} of Ca^{2+}-activated, voltage-dependent BK currents: consequences of rapid inactivation by a novel β subunit. *J. Neurosci.* **20:**4890–4903

Xia, X-M., Zeng, X., Lingle, C.J. 2002. Multiple regulatory sites in large-conductance calcium-activated potassium channels. *Nature* **418:**880–884

Zhang, X., Puil, E., Mathers, D.A. 1995. Effects of intracellular Mg^{2+} on the properties of large-conductance, Ca^{2+}-dependent K^+ channels in rat cerebrovascular smooth muscle cells. *J. Cereb. Blood Flow Metab.* **15:**1066–1074

Zhang, X., Solaro, C.R., Lingle, C.J. 2001. Allosteric regulation of BK channel gating by Ca^{2+} and Mg^{2+} through a nonselective, low affinity divalent cation site. *J. Gen. Physiol.* **118:**607–635

Zeng, X.H., Xia, X.M., Lingle, CJ. 2005. Divalent cation sensitivity of BK channel activation supports the existence of three distinct binding sites. *J. Gen. Physiol.* **125:**273–286